Title

Thermal volume change of poorly draining soils I: Critical assessment of volume change mechanisms

Authors
Coccia, Charles James Russell
McCartney, John S

Publication Date
2016-12-01

DOI
10.1016/j.compgeo.2016.06.009

Peer reviewed

Thermal Volume Change of Poorly Draining Soils
I: Critical Assessment of Volume Change Mechanisms

Charles James Russell Coccia, Ph.D., Research Associate
University of Colorado Boulder
Department of Civil, Environmental and Architectural Engineering
UCB 428, Boulder, CO 80309; coccia@colorado.edu
John S. McCartney, Ph.D., P.E., Associate Professor
University of California San Diego
Department of Structural Engineering
9500 Gilman Dr., La Jolla, CA 92093-0085; mccartney@ucsd.edu

ABSTRACT: The thermal volume change of soils is typically interpreted using the stress history and changes in yield stress with temperature (thermal softening). However, the path followed to reach a given stress history may lead to different thermal volume changes. Alternative mechanisms of thermal volume change are explored using data from the literature and isotropic, drained heating tests on compacted silt. No relationship between thermal volume change and degree of saturation was observed. However, a clear relationship with the secondary compression prior to heating was observed, indicating that thermally accelerated creep may provide better thermal volume change predictions than thermal softening.

KEYWORDS: thermal volume change, thermal creep, geothermal, constitutive modeling

INTRODUCTION

The thermal volume change behavior of saturated and unsaturated soils has gained interest in geotechnical engineering in recent years due to a wide range of applications involving temperature fluctuations (McCartney et al. 2016). Examples of such applications include energy piles (Brandl 2006; Laloui et al. 2006; Murphy and McCartney 2015), thermally-active soil embankments (Coccia and McCartney 2013), thermally-active retaining walls (Adam and Markiewicz 2009; Stewart et al. 2014), and radioactive waste storage systems (Gens 2001), among others. Experimental observations in the literature indicate increases in temperature may result in permanent changes in volume for saturated, fine-grained, poorly draining soils such as silts and clays (Campanella and Mitchell 1968, Demars and Charles 1982, Sultan et al. 2002, and Cekerevac and Laloui 2004) and unsaturated soils (Salager et al. 2008; Tang et al. 2008; Uchaipichat et al. 2009). Further, the stress history, quantified using the overconsolidation ratio (OCR), has been observed to play an important role in the magnitude and sign of the thermal volume change response. Specifically, during drained heating, normally consolidated soil will exhibit elasto-plastic thermal contraction (Campanella and Mitchell 1968; Cui et al. 2000; Delage et al. 2000; Cui et al. 2009; Uchaipichat and Khalili 2009), while heavily-overconsolidated soils exhibit elastic expansion (Cekerevac and Laloui 2004).

Possible mechanisms for the observed drained thermal plastic contraction in normally consolidated soils have been hypothesized to be due to the dissipation of thermally-induced excess pore water pressures resulting from the differential thermal expansion of the soil pore water and soil solids, thermal collapse of the soil skeleton due to the influence of temperature on the soil structure, and changes in viscosity of the pore fluid (Campanella and Mitchell 1968; Schiffman 1971). Based on the first mechanism, thermal consolidation is considered analogous to the primary consolidation of soils following a rapid increase in total stress (Campanella and Mitchell 1968). However, this mechanism does not fully clarify why overconsolidated soils will elastically expand and normally consolidated soils will plastically contract during heating. In addition, most semi-empirical thermo-elasto-plastic models disregard this explanation for thermal volume change, and instead have developed empirical relationships based on the influence of stress history (i.e., the magnitude of OCR) observed in the literature. This is typically achieved through the incorporation of a thermal softening function into the yield surface or mean preconsolidation stress value (Laloui and Cekerevac 2003). Although the elasto-plastic models built upon thermal softening mechanisms provide reasonable predictions of the thermal volume change of soil of different stress states (e.g., Cui et al. 2000; Laloui and Cekerevac 2003), a drawback is a lack of consideration for the time-dependency of thermal consolidation (Towhata et al. 1993; Burghignoli et al. 2000) as well as a lack of a physics-based explanation for plastic thermal volume change. Further, these thermo-elasto-plastic constitutive models typically require an extensive soil-specific thermo-hydro-mechanical testing program for calibration, requiring thermal soil testing equipment not typically available in most geotechnical labs.

On the other hand, experimental evidence also supports the hypothesis that the thermal volume change of fine-grained, poorly-draining soils may be indirectly influenced by the OCR because of accelerated secondary (creep) deformations resulting from the most recent change in effective stress prior to heating (Towhata et al. 1993; Burghignoli et al. 2000). Specifically, the soil's transient creep behavior due to recent mechanical loading or unloading prior to heating may impact the sign (contraction or expansion) and magnitude of drained thermal volume change. Thermal volumetric contraction has been observed for normally and overly-consolidated soils if the rate of secondary compression was positive (indicating decreasing volume) before heating, while thermal volumetric expansion has been observed if the rate of secondary compression was negative before heating (Towhata et al. 1993; Burghignoli et al. 2000).

This study focuses on an alternative explanation for the underlying mechanism of thermal volume change of saturated and unsaturated soils, specifically an acceleration of the secondary compression process that was ongoing in the soil before experiencing a change in temperature. This paper seeks to establish that this explanation can be used to interpret the thermal volume change response of saturated and unsaturated soils based on use of the secondary compression index to define the thermally accelerated creep deformation, and that it can clarify the difference in behavior noted for soils with different stress histories. To investigate the underlying mechanisms responsible for the thermal volume change response of saturated and unsaturated soils, experimental results from the literature must be summarized. In particular, the findings of Burghignoli et al. (2000) and Towhata et al. (1993) are critically assessed to highlight the drawbacks of assuming thermal volume change to be primarily dependent on overconsolidation ratio. In addition, an experimental testing program was carried out to assess the thermal volume change mechanisms of compacted Bonny silt at different degrees of saturation, paying attention to the secondary compression response prior to heating. The results of the experimental program are used to highlight the influence of thermally-accelerated creep on thermal volume change, along with the potential role of the degree of saturation on thermal volume change.

In a companion paper (Coccia and McCartney 2016a), a critical assessment of current elasto-plastic models that primarily rely on the thermal softening behavior for thermal volume change predictions is provided. Further, the drawbacks of these thermal constitutive models are revealed based on the results of Burghignoli et al. (2000) and Towhata et al. (1993), and a new constitutive model applicable to both saturated and unsaturated soils is presented. Finally, the thermal volume change results for unsaturated Bonny silt as well as those for a saturated clay under different stress histories presented by Towhata et al. (1993) are used to validate the proposed model.

THERMO-MECHANICAL RESPONSE OF POORLY DRAINING SOILS

Thermal Volume Change Behavior

It is well-established in the literature that overconsolidated, poorly-draining soils prepared by unloading from a normally consolidated state tend to expand during drained heating, while the same soils under normally consolidated conditions tend to contract during drained heating. Cekerevac and Laloui (2004) performed drained heating tests on Kaolinite clay (PI = 21, USCS classification of CL) between 22 and 90 °C at different OCRs using a temperature-controlled triaxial cell. The thermally induced volumetric strain with temperature observed by Cekerevac and Laloui (2004) for specimens with different OCRs is shown in Figure 1(a), where contraction is considered positive. Thermal contraction was observed for OCRs of 1.0, 1.5, and 2.0 while thermal expansion followed by contraction was measured for OCRs of 6.0 and 12.0. Further, the magnitude of initial thermal expansion is observed to increase with increasing OCR. Similar behavior has also been observed by Abuel-Naga et al. (2007). On the other hand, Sultan et al. (2002) performed drained heating tests on undisturbed samples of Boom clay and observed the initial thermal expansion during heating to be equal in magnitude for overconsolidation ratios ranging from 2 to 12. The impact of stress history, as defined by the OCR, on the initial thermal volumetric strain rate of different soils is summarized in Figure 1(b).

Baldi et al. (1988) was the first to observe that overconsolidated soils will transition from expansion to contraction when heated beyond a unique temperature, referred to as the "transition temperature". For example, the results in Figure 1(a) show that a Kaolinite clay specimen with an OCR of 12 will expand until achieving a change in temperature of 28 °C, after which it starts to contract for higher changes in temperature. Similarly, the specimen having an OCR of 1.5 exhibited thermal expansion up to a change in temperature of around 8 °C, after which thermal contraction followed. This transition from thermal expansion to contraction has been observed in other studies as well (Towhata et al. 1993; Sultan et al. 2002; Cekerevac et al. 2004). The transition temperature tends to increase with increasing OCR, as shown in Figure 2 for various clays.

During cooling, a relatively linear thermal contraction is typically observed regardless of the OCR (Baldi et al. 1991; Abuel-Naga et al. 2007; Uchaipichat and Khalili 2009; Coccia and McCartney 2012), although thermal expansion during cooling has been observed in some cases (Campanella and Mitchell 1968; Baldi et al. 1986). The difference in behavior between heating and cooling of normally consolidated clay reveals an irreversible contraction at the end of a heating-cooling cycle. Cui et al. (2000) postulated that heating above the maximum temperature previously applied to the soil would lead to irreversible plastic thermal strains. Demars and Charles (1982) found that the magnitude of thermally induced plastic strain of normally consolidated soils during initial heating is independent of the applied stress. This was also observed by Abuel-Naga et al. (2007), who found the initial void ratio does not have an impact on the thermal volume change response of soil having any value of OCR.

Fewer studies have focused on the drained thermal volume change of unsaturated soils (Romero et al. 2003; Salager et al. 2008; Tang et al. 2008; Uchaipichat and Khalili 2009). Furthermore, most of these studies were performed on compacted, expansive clays or clays having very high OCRs. Data from the literature suggests the thermal response of unsaturated soils to be similar to that of saturated soils (Romero et al. 2005; Uchaipichat and Khalili 2009). Uchaipichat and Khalili (2009) performed drained heating tests on three compacted silt specimens of different initial suction values (0, 100, and 300 kPa) at four different values of net confining stress (50, 100, 150, and 200 kPa) to assess the influence of suction and confining stress on thermally induced strain. Thermal expansion was observed to occur for specimens under lower net confining stresses (i.e. higher overconsolidation ratio) with the introduction of larger irreversible thermal contraction with increasing net stress (and decreasing OCR), as observed in Figure 3. For a given net stress, the results in Figure 3 indicate that the amount of thermal contraction increases with suction, with the impact of unsaturated conditions having a more prominent effect at lower values of net stress.

Based on the definition of generalized effective stress of Bishop (1959):

$$p' = (p - u_a) + \chi(u_a - u_w) \qquad \text{EQ. 1}$$

where p is mean total stress, u_a is the pore air pressure, u_w is the pore water pressure, and χ is the effective stress parameter used to define the influence of matric suction on mean effective stress, the impact of suction on the thermal volume change behavior observed by Uchaipichat and Khalili (2009) may be assessed. As suction increases, the mean effective stress increases following EQ. 1. Uchaipichat and Khalili (2009) found that the mean effective preconsolidation stress of the soil also increases with suction, albeit to a lesser extent. This means that the OCR will decrease during an increase in suction and may cause the specimen to have a thermal response similar to that of a normally consolidated soil. Salager et al. (2008) performed drained heating tests on six specimens of compacted Sion silt under different applied suctions (50, 100, and 300 kPa) and a net mean stress of 50 kPa. Suction was concluded to have no significant effect on thermally induced volumetric strain based on the experimental results. When interpreted in terms of overconsolidation ratio, based on mean effective stress defined assuming that $\chi = S$, the data from Uchaipichat and Khalili (2009) and Salager et al. (2008) indicate the impact of OCR on thermal volume change as shown in Figure 4. However, there is no clear influence of matric suction aside from its contribution to the soil mean effective stress and preconsolidation stress.

Possible Mechanisms of Thermal Volume Change

The thermally induced volume change behavior of saturated soils under drained conditions has been associated with three unique mechanisms that either contribute to or affect the observed recoverable or irrecoverable volume change response of soil during drained heating (Paaswell 1967; Campanella and Mitchell 1968; Delage et al. 2000; among others). The first and primary mechanism, as described by Campanella and Mitchell (1968) and Delage et al. (2000), occurs due to the thermal expansion of the soil solids and soil pore water. During heating, the individual constituents of a bulk material will expand elastically with time and temperature. Due to the differences in the coefficients of thermal expansion of the water and soil solids, a differential expansion will occur among the soil constituents leading to thermal pressurization. Depending on the soil mineralogy, water can expand by as much as 7 to 12 times more than the soil solids (McKinstry 1965).

The expansion of the soil constituents may result in two distinctive responses of the bulk soil. First, the elastic expansion of the soil minerals and pore water (and pore air for the case of unsaturated soils) will trigger a reversible bulk thermal expansion of the affected soil (Campanella and Mitchell 1968; Uchaipichat and Khalili 2009). This phenomenon has been attributed to be responsible for the thermal volumetric expansion observed for highly overconsolidated soils during heating as well as the linear thermal contraction observed during cooling for all soils following heating (Cui et al. 2000; François and Laloui 2008; among others). Second, the differential expansion between the pore water and soil solids may cause a generation of excess pore water pressure within the soil if heated in undrained conditions (Ghaaowd et al. 2016) or in drained conditions when the rate of heating is faster than the rate of drainage of water from the soil, thereby introducing a temporary undrained condition. In drained conditions, the excess pore water pressure will dissipate with time as a function of the soil's permeability, causing a flow of pore water toward the drainage boundaries. This drainage results in a time-dependent, volumetric contraction of the soil as the pore water pressure continues to dissipate (Campanella and Mitchell 1968; Booker and Savvidou 1985). Campanella and Mitchell (1968) relates this phenomenon to the primary consolidation behavior observed in stress-induced consolidation and is generally referred to as thermal primary consolidation (Houston et al. 1985; Burghignoli et al. 2000). It is important to note that the significance of this mechanism is highly dependent on the rate of heating and soil hydraulic conductivity. Specifically, as the generation of excess pore water pressure is dependent on the ability for the pore water to flow from the soil, different heating rates can result in a difference in the thermal volume change response dependent on the mechanisms activated as well as the extent of thermally induced excess pore water pressure (Sultan 1997). Further, the permeability of the soil can influence the resulting thermal volume change mechanisms. For example, sandy soils are expected to exhibit a less significant increase in excess pore water pressure during heating due to the enhanced ability for the pore water to flow from the void space (Noorishad et al. 1984).

The second mechanism described by Campanella and Mitchell (1968) is a decrease in inter-particle shearing strength due to an increase in temperature. This decrease may be a result of the increase in thermal energy due to heating, resulting in a collapse of the soil skeleton, ultimately reducing the void ratio of the specimen. This has been described to be analogous to secondary compression behavior observed after mechanical primary consolidation and is referred to as "thermal secondary compression". This process continues until enough new bonds are developed that can carry the thermo-mechanically induced stresses. This process is typically considered to be irreversible since no additional inter-particle bonds are necessary to carry the stresses resulting from a subsequent cooling cycle (Campanella and Mitchell 1968).

The third contributing mechanism of thermally induced volume change, described by Paaswell (1967), is the effect of a decrease in pore water viscosity with increasing temperature. Lower fluid viscosities will result in an increase in the permeability of the soil. This phenomenon can be described by the Kozeny-Carman equation, given as follows (Mitchell and Soga 2005):

$$k_s = k_p \left(\frac{\gamma_w}{\eta_d}\right) \qquad \text{EQ. 1}$$

where k_p is the intrinsic permeability, η_d is the dynamic viscosity of water, and γ_w is the unit weight of water. From this third mechanism, an increased rate of thermally-induced volume change is expected during heating at higher temperatures due to the ability of the pore water to flow through the soil with less resistance. This behavior was observed by Towhata et al. (1993) who performed consolidation tests at different temperatures for a loading increment from 80 to 160 kPa to assess the impact of temperature on the time rate consolidation behavior of MC clay. Although all four specimens were observed to achieve the same final void ratio, specimens at higher temperatures were observed to consolidate at a much faster rate (Figure 5). This behavior has also been observed by Delage et al. (2000). Finally, this decrease in dynamic fluid viscosity may also contribute to the decrease in inter-particle shearing strength responsible for collapse of the soil skeleton during thermal secondary compression.

The relative contributions of these mechanisms may be assessed experimentally by evaluating the results from thermal consolidation tests performed under undrained and then drained conditions. A hypothetical stress path for such a thermal consolidation test is shown in

Figure 6, where a soil specimen is first heated in undrained conditions (Path 1), resulting in the development of thermally-induced excess pore water pressures [Figure 6(a)]. This may result in an increase in void ratio due to the thermal expansion of the soil constituents as shown in Figure 6(b), as well as a decrease in p'. Next, drainage of the soil pore water is allowed, resulting in the dissipation of thermally induced excess pore water pressure from the previous undrained heating step. This results in an increase in p' to p'_{target} as seen in Figure 6(a) for Path 2 and 3. During this time, the thermal primary consolidation stage (Path 2) and the thermal secondary compression stage (Path 3) may be observed before and after the excess pore water pressures have fully dissipated ($\Delta u_w = 0$), respectively as shown in Figure 6(b).

Houston et al. (1985) performed thermal consolidation tests on undisturbed saturated specimens of Pacific Illite and Pacific Smectite. During undrained heating, a generation of thermally induced excess pore water pressure was observed to develop as a function of the initial soil temperature and mean effective confining stress. As a result, the soil first exhibited a slight volumetric expansion due to the thermal expansion of the soil constituents (in this case, the soil solids and pore water) and the decrease in mean effective stress. Next, drainage was allowed causing the excess pore water pressure to dissipate in a time-dependent manner resulting in volumetric contraction of the specimen. Once all excess pore water pressure had dissipated, the soil continued to deform under constant mean effective stress. During the process of secondary thermal compression, Houston et al. (1985) observed the coefficient of secondary compression, $C_{\alpha\varepsilon}$, to increase linearly with increasing temperature as shown in Figure 7, where $C_{\alpha\varepsilon}$ is the volumetric strain per log time.

Unlike the deformations observed during mechanical consolidation, Houston et al. (1985) observed that the deformations due to thermal secondary compression were much larger than the contraction resulting from the dissipation of thermally induced excess pore water pressures during thermal primary consolidation, thereby dominating the overall thermal volume change process. The results of the study by Houston et al. (1985) suggests the primary mechanism of thermal volume change to be due to the viscous deformation of the soil structure in response to an increase in temperature, and not the volume change response associated with the dissipation of thermally induced excess pore water pressure.

Similar results were observed by Burghignoli et al. (2000), who performed thermal consolidation tests on specimens of reconstituted specimens of Todi clay and undisturbed samples of Fiumicino clay. The volume change results of three thermal consolidation tests are shown in Figure 8. For Test TD12, a reconstituted specimen of Todi clay was loaded to normally consolidated conditions at a mean effective stress of 190 kPa. After loading, the specimen was heated in undrained conditions from 30 to 40 °C. During heating, an increase in excess pore water pressure was observed, along with a slight increase in void ratio (≈ 0.003). The measured relationship between the thermally induced excess pore water pressure and corresponding change in void ratio shows the soil to follow below the unloading-reloading curve as seen in Figure 8(a). Once the excess pore water pressure stabilized, drainage was opened to allow the excess pore water pressures to dissipate. Similar to the results of Houston et al. (1985), the soil specimen was observed to contract in both primary and secondary stages of thermal consolidation and compression. During thermal primary consolidation, the soil void ratio decreased from 0.893 to 0.885. Following, the soil continued to deform under thermal secondary compression at constant mean effective stress to a final void ratio of 0.880 [Figure 8(a)]. Considering an initial void ratio of 0.89 prior to undrained heating, primary consolidation appears to contribute to 50% of the overall thermal volume change due to the increase in temperature to 40 °C for the first temperature increment of Test TD12 [Figure 8(a)]. Once thermal contraction began to stabilize, the drains were closed once again and the soil was heated from 40 to 48 °C. Similar to the first heating step, a decrease in mean effective stress was observed along with an increase in void ratio. During the following drainage phase, a similar magnitude of thermal contraction during thermal primary consolidation was observed. However, a slightly smaller reduction in volume due to thermal secondary compression was reported for the second temperature increment [Figure 8(a)]. For both temperature steps in Test TD12, the stress-strain relationship during undrained heating and drained thermal primary consolidation appears to follow a hysteretic curve similar to that typically observed for a mechanical unloading-reloading cycle. In addition, the contribution of thermal primary consolidation appears to be heavily dependent on the hysteretic nature of the unloading-reloading cycle.

Had the soil tested by Burghignoli et al. (2000) been heated under drained conditions at a slow heating rate, the contribution of thermal primary consolidation may have been expected to decrease, permitting thermal secondary compression to significantly dominate the overall thermal volume change response as was observed by Houston et al. (1985). Furthermore, Burghignoli et al. (2000) indicated the rate of thermal secondary compression to remain significant following the end of data collection for each test. As such, the true contribution of thermal secondary compression may be larger than reported in Figure 8(a). Burghignoli et al. (2000) performed a thermal consolidation test on an undisturbed sample of Fiumicino clay in normally consolidated conditions as well. Similar to the Todi clay, the sample was observed to expand during undrained heating along the elastic unloading path, and then contract during both the primary and secondary stages of thermal consolidation during drainage, as shown in Figure 8(b).

Burghignoli et al. (2000) also performed a thermal consolidation test on a reconstituted specimen of Todi clay unloaded to an overconsolidation ratio of 4 as shown in Figure 8(c). During undrained heating from 30 to 40 °C, an increase in excess pore water pressure was observed, resulting in a reduction of mean effective stress and an increase in volume along the elastic unloading path followed during the previous mechanical unloading increment. Following heating, the excess pore water pressure was observed to dissipate while still in undrained conditions. The dissipation of pore water pressure is the result of the tendency of the soil to exhibit expansive secondary creep due to the mechanical unloading increment performed prior to undrained heating. Dissipation of the excess pore water pressure caused a "reloading" of the soil following the elastic reloading curve, as shown in Figure 8(c). Eventually the drainage was opened and any remaining excess pore water pressure was allowed to dissipate. Overall, an increase in void ratio was observed following undrained heating and drained consolidation. This increase in void ratio appears to be due to the hysteretic nature of the unloading-reloading path. Following the thermal consolidation heating test, Burghignoli et al. (2000) cooled the specimen from 39 to 30 °C in undrained conditions. Undrained cooling resulted in the development of negative excess pore water pressures causing an increase in mean effective stress. A slight decrease in soil volume was observed during cooling along the elastic reloading path, as shown in Figure 8(c). During the drainage phase, the soil volume-effective stress returned to the initial conditions prior to cooling resulting in a negligible overall change in void ratio. As observed in Figure 8(c), little to no contribution from thermal secondary compression is observed for the overconsolidated Todi clay. Burghignoli et al. (2000) attributed this response to the reduction in secondary compression behavior achieved during unloading to the target overconsolidation ratio, similar to the method of load surcharging to reduce long-term soil settlement (Mesri and Feng 1991).

Impact of Recent Stress History on Secondary Compression and Thermal Volume Change

Results from the literature have generally indicated thermal volume change to be primarily dependent on the overconsolidation ratio prior to heating (Campanella and Mitchell 1968; Cui et al. 2000; Delage et al. 2000; Cui et al. 2009; Uchaipichat and Khalili 2009). However, this observed phenomenon may be a result of the experimental procedures utilized during testing (i.e., loading to achieve NC conditions and unloading to achieve OC conditions) and may not truly describe the soil behavior. Instead, the secondary compression behavior following a recent change in total or effective stress may be more indicative of the thermal volume change response. Drained thermal volume change tests were performed on normally consolidated and overly consolidated saturated specimens of Todi clay, Fiumicino clay, and Bologna clay by Burghignoli et al. (2000), and MC clay by Towhata et al. (1993) to investigate the impact of recent stress history on resulting thermal volumetric strain. Overconsolidated stress states were achieved via two different techniques: 1) by unloading the specimen to the target OCR (UL approach), and; 2) by unloading past the target OCR and then reloading to the target OCR (RL approach). This procedure is summarized in Figure 9. Comparison of two overconsolidated soils achieved by either the RL or UL approach shows the final overconsolidation ratio to be equal (shown in Figure 9); however, the direction of the most recent change in effective stress is opposite.

The total changes in void ratio during heating, Δe_{total}, recorded from these studies have been divided by the applied change in temperature, ΔT, and plotted against the initial overconsolidation ratio, prior to heating, for the normally consolidated specimens and recently unloaded (UL) overconsolidated specimens in Figure 10(a), where a positive change in void ratio with change in temperature signifies contraction. Similar to the behavior in Figures 1(b) and 4, the thermal volume change behavior is observed to transition from contraction to expansion with increasing overconsolidation ratio.

In Figure 10(b), the change in void ratio with change in temperature for the recently reloaded (RL) overconsolidated specimens has been included with the results from Figure 10(a). A clear impact of the recent stress history (i.e. recent direction of loading) is observed in Figure 10(b) where all reloaded OC specimens exhibited thermal contraction and most unloaded OC specimens exhibited thermal expansion during an increase in temperature. In Figure 10(b), the magnitude of thermal volume change is observed to decrease with increasing OCR. However, this decrease is not as significant as that observed in Figures 1(b), 4, or 11(a) for overconsolidated specimens prepared via unloading. These results suggest the thermal volume change response of soil to be more dependent on the path taken to obtain a given stress history, than on OCR alone.

EXPERIMENTAL INVESTIGATION

The results of Burghignoli et al. (2000) and Towhata et al. (1993) suggest the thermal volume change response of soil to be more dependent on the recent stress history (loading vs. unloading), than on OCR alone. Also, the role of unsaturated soils during thermal volume change remains unclear without the accompanied influence of OCR. As such, an experimental testing program was carried out to assess the thermal volume change mechanisms of compacted Bonny silt at different degrees of saturation, paying attention to the secondary compression response prior to heating, as well as the evolution of degree of saturation during heating.

Material and Specimen Preparation

The thermal volume change behavior of compacted specimens of soil collected from the Bonny dam located near the Colorado/Kansas border in Yuma County, CO referred to as Bonny silt was evaluated in this study. A summary of the relevant geotechnical properties for the soil are provided in Table 1. The soil is classified as ML (inorganic low plasticity silt) according to the Unified Soil Classification System (USCS, ASTM D2487). An activity of 0.29 indicates the silt does not contain a significant amount of active clay minerals.

The silt specimens in this study were prepared to a dry density of approximately 1450 kg/m^3 (void ratio of approximately 0.83) at a target compaction gravimetric water content of 14.0% using static compaction. Specifically, a pneumatic piston was used to compress the specimen in one 27 mm-tall lift within a 67.1 mm-diameter cylindrical aluminum mold. After extraction of the specimen from the mold, it was weighed and its dimensions were measured to determine the obtained initial conditions. The compaction conditions evaluated in this study are different than those of previous studies that evaluated the behavior of compacted Bonny silt: Khosravi and McCartney (2011) used a void ratio of 0.53 and a compaction water content of 14%, Coccia and McCartney (2012) used a void ratio of approximately 0.46 and a compaction water content of 17.4%, and Alsherif and McCartney (2013, 2015) used a void ratio of 0.68 and a compaction gravimetric water content of 10.5%. The different compaction conditions are expected to lead to different hydraulic and mechanical properties.

Experimental Equipment

A high pressure thermal isotropic cell capable of independently controlling and monitoring net cell pressure, pore water pressure, pore air pressure, and temperature while measuring changes in net cell pressure, pore water volume, soil total volume, and temperature during testing was utilized to assess the thermal volume change mechanisms of saturated and unsaturated compacted Bonny silt (Coccia 2015; Coccia and McCartney 2016). A schematic of the isotropic cell is shown in Figure 11. The cell is designed to accommodate specimens having a height of 25.4 mm and a diameter up to 71.12 mm and can tolerate cell pressures up to 10 MPa. The cell pressure is controlled using a high pressure (CELL) flow pump and is monitored by a pressure sensor installed at the base of the isotropic cell (Figure 11). Matric suction of the soil specimen is controlled via the axis-translation technique (Hilf 1956). Specifically, pore air pressure is distributed to the top of the specimen through a 6.45 mm-thick, 71.1 mm-diameter coarse porous stone placed at the top of the soil specimen, while a pore water pressure (PWP) flow pump applies pore water pressure to the bottom of the specimen through a 7 mm-thick, 71.1 mm-diameter 1-bar high air entry value (HAEV) ceramic disk. Additional details on the program operation used to dry or wet the soil specimen can be found in Lee and Znidarčić (2013).

Changes in the soil volume are determined directly using three non-contact proximity probes installed within the isotropic cell chamber (Figure 11). Three steel targets adhered to the specimen are used to determine distances between the probe tips and the soil specimen. Two radially-oriented proximity probes are mounted at mid height to monitor changes in specimen diameter during testing. Two radial probes were used for redundancy as well as to assess the uniformity of deformation of the soil specimen. The third vertically-oriented proximity probe is mounted above the soil top cap to monitor changes in height. To ensure accurate changes in specimen height and diameter were determined during testing, an extensive calibration procedure was pursued to characterize the thermo-mechanical "machine" deformations of the isotropic cell equipment. Details of the thermo-mechanical calibration results may be found in Coccia and McCartney (2016b). The volumetric strain of the soil under various loading conditions is calculated using the averaged radial displacements recorded from the two radial probes and the vertical displacement recorded from the axial probe.

Changes in temperature are applied to the soil specimen by varying the temperature of the cell fluid located within the isotropic cell. The temperature of the cell fluid and soil specimen is regulated by circulating water through a 6.3 mm-diameter copper heating coil, installed within the cell chamber, that is heated using a heat pump. The temperature control system also permits the precise ramping of temperature within the cell, allowing for the application of slow temperature rates of less than 0.3 °C/hr. Sultan et al. (2002) observed this rate to be acceptable to ensure full drainage of saturated clay specimens during heating. The temperature of the cell fluid is monitored and recorded using two Omega K-Type thermocouples mounted at the top and bottom of the isotropic cell. To minimize the temperature gradient, a circulatory fan is mounted at the top of the isotropic cell is used to circulate the cell fluid within the cell chamber (Figure 11). To minimize heat loss during testing, the aluminum isotropic cylinder is wrapped with two layers of 6.35 mm-thick thermal insulation. Further details of the experimental setup may be found in Coccia and McCartney (2016b).

Experimental Procedures

Following compaction, the soil specimen was placed into the isotropic cell atop the bottom cap and 1-bar ceramic disk. The soil top cap and coarse stone was then placed atop the soil specimen and the neoprene membrane was placed around the specimen. A vacuum of 81.5 kPa was applied to the top of the specimen to de-air the soil and seat the membrane. Next, the displacement probes and accompanying brackets were installed. The remaining components of the isotropic cell were then assembled, the cell chamber was filled with de-aired mineral oil, and a seating confining stress of 50 kPa was applied. Next, the top vacuum was reduced to 68 kPa and de-aired water was flushed upwards from the bottom of the specimen by imposing a pore water pressure of 20 kPa. De-aired water was flushed upward through the soil specimen until a volume of water equivalent to two pore volumes had passed through the soil and air bubbles were no longer observed coming from the top of the soil specimen, which on average took 5-6 hours. The vacuum at the top of the specimen was turned off and switched to a pore water pressure of 20 kPa equal to that applied at the bottom of the soil specimen. The total stress (50 kPa) and backpressure (20 kPa) were increased in stages of 35 kPa until a total stress of 350 kPa and a backpressure of 320 kPa was achieved. The compacted specimen was not observed to exhibit any significant change in volume during this process. The soil was left to backpressure saturate overnight. This technique was observed to achieve an average B-value of around 0.96, and was considered sufficient for saturation.

Following backpressure saturation, the remainder of the experimental testing of the compacted silt was carried out in three distinct stages: (1) matric suction application; (2) isotropic compression under a constant rate of strain to a target mean total stress of 1000 kPa; and (3) drained heating. In total, five tests were performed to assess the thermal volume change mechanisms of compacted silt. The soil conditions following initial compaction for the five tests are summarized in Table 2. Tests S-0 was performed to establish the thermal volume change response for the saturated compact silt during heating and cooling. Next, Tests US-15, US-20, US-30, and US-40 were performed to establish the influence of the rate of secondary deformation and degree of saturation, achieved via an applied matric suction of 15, 20, 30, and 40 kPa, respectively, on thermal volume change during heating. The thermo-hydro-mechanical stress paths followed for the five tests are summarized in Figure 12. In Figure 12, the “saturated path” was followed for Test S-0, while the “unsaturated path” was followed for Tests US-15, US-20, US-30, and US-40. The procedures for testing the specimens following saturation are as follows:

1. Application of matric suction of 10*, 15*, 20, 30, and 40 kPa for Tests US-15, US-20, US-30, and US-40, respectively, using the PWP flow pump. Pore water was removed from the soil specimen by withdrawing the piston of the PWP flow pump at a rate of 0.0001 mm/s which corresponds to an apparent Darcy velocity of 2.23×10^{-8} m/s (500 times smaller than the saturated hydraulic conductivity of the silt). The degree of saturation of the soil was assumed to reach equilibrium after the PWP flow pump remained off for longer than 5000 seconds. *Prior to the application of 15 kPa matric suction to the compacted specimen for Test US-15, an intermediate suction of 10 kPa was applied to the specimen to assess the soil water retention relationship at lower degrees of matric suction.
2. Mechanical isotropic compression of the specimens for Tests S-0, US-15, US-20, US-30, and US-40 to a mean total stress of 1000 kPa, equivalent to a mean net stress of 680 kPa. A mean total stress of 1000 kPa was selected as it is large enough to achieve normally consolidated conditions for the soil specimen so that the mean effective preconsolidation stress may be properly defined. Specimens were loaded in constant rate of strain conditions with a constant cell flow pump piston velocity of 4×10^{-5} for Tests S-0A/B, Test US-20, and Test US-40, and 2×10^{-5} mm/s for Test US-30. This corresponds to apparent strain rates of 0.173 and 0.086 %/hr, respectively. The apparent strain rate includes both soil and machine deformations. A slow loading rate was used to minimize the generation of excess pore water pressure during loading so that the equilibrium compression curve of the soil may be characterized.
3. Drained heating of Tests S-0, US-15, US-20, US-30, and US-40 to a target temperature of 65 °C at a rate of 0.35 °C/hr. Heating was performed in three stages from ambient temperature

to an observed ≈ 35 °C, 35 to ≈ 48 °C, and 48 °C to ≈ 63 °C, and the temperature was held until equilibrium was reached at each stage. Following heating in Test S-0, a cooling step was performed to ambient temperature to assess the additional thermal volume change response.

Experimental Results

For interpretation of the test results in this study, the mean effective stress was calculated using the definition of generalized effective stress proposed by Bishop and Blight (1963), where the effective stress parameter, χ, is assumed equal to the degree of saturation, S, as follows:

$$p' = (p - u_a) + S(u_a - u_w) \quad \text{EQ. 2}$$

EQ. 2 may be rewritten as:

$$p' = p_{net} - S\psi \quad \text{EQ. 3}$$

where p_{net} is the difference between the mean total stress and the pore air pressure, and ψ is matric suction.

For all drained heating and/or cooling tests, the thermal expansion/contraction of the soil solids and soil pore water has been considered for the calculation of changes in void ratio and degree of saturation. Specifically, the change in pore volume (ΔV_v) and change in volume of soil pore water (ΔV_w), has been modified to account for thermal expansion. Throughout testing, changes in volume of the soil specimen are deduced based on deformations in the radial and axial directions. During heating or cooling, the measured change in volume ($\Delta V_{t,measured}$) is assumed to be a summation of the change in volume of the voids and the thermal expansion (or contraction) of the soil solids:

$$\Delta V_{t,measured} = \Delta V_v + V_{s0}\alpha_{T,s}\Delta T \quad \text{EQ. 4}$$

where V_{s0} is the initial volume of the soil solids, and $\alpha_{T,s}$ is the thermal coefficient of volumetric expansion of the soil solids. For this study, $\alpha_{T,s}$ is assumed to be 3.5×10^{-5} 1/°C, as specified by Campanella and Mitchell (1968). The resulting change in pore volume during a change in temperature may be written as:

$$\Delta V_v(\Delta T) = \Delta V_{t,measured} - V_{s0}\alpha_{T,s}\Delta T \qquad \text{EQ. 5}$$

Likewise, the change in volume of the soil pore water during heating or cooling must also be considered. Campanella and Mitchell (1968) proposed the following relationship considering the properties of free pure water:

$$\Delta V_w(\Delta T) = \Delta V_{w,measured} - V_{w0}\alpha_{T,w}\Delta T \qquad \text{EQ. 6}$$

where $\Delta V_{w,measured}$ is the change in water volume measured by the PWP flow pump, and $\alpha_{T,w}$ is the thermal coefficient of volumetric expansion of the pore water, assumed to be equal to 2.07×10^{-4} 1/°C. Baldi et al. (1988) proposed a modification to EQ. 6 to incorporate the effects of adsorbed water using the double layer theory for low porosity plastic clays. However, Delage et al. (2000) found the assumption of free water by Campanella and Mitchell (1968) to be sufficient for the evaluation of the thermal volume change of the pure water in Boom clay so this assumption was followed in this study.

The results from the suction application stage for Tests US-15, US-20, US-30, and US-40 are shown in Figure 13 in terms of the final degree of saturation and accompanying matric suction measured at equilibrium. During the application of matric suction, the degree of saturation was observed to decrease with increases in matric suction. The final values of matric suction and degree of saturation are summarized in Table 3. The Brooks and Corey (1964) SWRC model was selected to provide a functional relationship for the SWRC data from the axis translation tests in this study (Tests US-15, US-20, US-30, and US-40), and is given as follows:

$$S = S_r + (S_s - S_r)\left(\frac{\psi_{ae}}{\psi}\right)^{\lambda_{BC}} \qquad \text{EQ. 7}$$

where S_s is the degree of saturation determined at $\psi = 0$ (equal to 1 prior to initial drying of a saturated soil), S_r is the residual degree of saturation, ψ_{ae} is the air entry suction, and λ_{BC} is a fitting parameter related to the pore size distribution. The SWRC fit is shown with the results from Tests US-15, US-20, US-30, and US-40 in Figure 13. The parameters ψ_{ae} and λ_{BC} were determined using least squares minimization and a residual degree of saturation of 0.35 was observed. Two additional data points from preliminary drying-path tests are included in Figure 13 to confirm the repeatability of the suction application procedures at matric suctions of 30 and 40 kPa (Coccia 2015). Overall, the fitted SWRC model corresponds well with the experimentally determined suction-saturation values from this study.

Following achievement of the target matric suction, the soil specimens were loaded to a mean total stress of 1000 kPa. The volume change results for all five tests are summarized in Figure 14(a) in terms of the decrease in void ratio against the mean effective stress, where a positive change in void ratio indicates compression. A shift in the compression curves towards larger values of mean effective stress was observed with increasing matric suction and decreasing degree of saturation, and the compression curves are approximately parallel suggesting the slope of the virgin compression line to be unaffected by changes in matric suction and/or degree of saturation for the range of stresses investigated in this study. This behavior was also observed by Uchaipichat and Khalili (2009), among others. Following completion of mechanical loading to 1000 kPa, the soil specimens were observed to continuously deform at a slow rate under constant mean effective stress as a result of secondary compression. This behavior may be seen in Figure 14(a) as a vertical tail at the end of each compression curve. The measured degree of saturation with mean effective stress during loading for Tests US-15, US-20, US-30, and US-40 is summarized in Figure 14(b). The degree of saturation did not change significantly until reaching the yield stress, after which an increase is observed with increasing mean effective stress. This behavior suggests plastic changes in void ratio are necessary to induce an increase in degree of saturation during mechanical loading. Further discussion of the drained mechanical loading results and analysis can be found in Coccia (2015) and Mun et al. (2016).

Results from the drained heating tests on the compacted silt are shown in Figure 15. Heating was initiated for each test once the observed volumetric strain rate from the previous isotropic mechanical loading stage was less than 0.0005 %/hr. A maximum heating rate of 0.34 °C/hour was applied for all tests. The total change in void ratio with temperature is shown in Figure 15(a) for all tests. All soil specimens exhibited contraction with increases in temperature as expected for a soil heated in normally consolidated conditions (Cekerevac and Laloui 2004). Furthermore, the magnitude of thermal volume change measured in this study is in agreement with that observed for other soils of similar plasticity (Coccia and McCartney 2016b). During heating, a slight decrease in degree of saturation was observed to occur for all the unsaturated specimens, as observed in Figure 15(b).

Analysis

During mechanical loading, a change of degree of saturation may occur as observed in Figure 14(b). Specifically, increases in effective stress will result in a decrease in void ratio [Figure 14(a)] causing an increase in the air entry suction. This occurs as a higher value of matric suction will be required to introduce air into the reduced pore network (Kawai et al. 2000). The influence of mechanical loading on the SWRC for Bonny silt is shown in Figure 16(a). During mechanical compression, the air entry suction was observed to increase slightly to 9.1 kPa as a result of decreases in void ratio ranging from 0.08 to 0.12 [Figure 14(a)]. Likewise, during heating a change in degree of saturation is also expected to occur due to the accumulative influences of changes in void ratio and increases in temperature. While decreases in the void ratio will cause an increase in the air entry value, increases in temperature will induce a decrease in the air entry suction. This is due to a decrease in viscosity of the pore water resulting in a reduction in interfacial tension between the pore water and soil solids, thus requiring a smaller value of suction to introduce air into the pore system (Romero et al. 2001). For the Bonny silt, heating was observed to reduce the air entry suction to a value of 8.9 kPa [Figure 16(a)]. This decrease in degree of saturation for all tests during heating suggests the impact of temperature on the air entry suction to dominate the adjoined effect of the decrease in void ratio for this study. This behavior has also been observed by Uchaipichat and Khalili (2009) for compacted Bourke silt.

Moreover, decreases in degree of saturation observed during heating are expected to cause an increase in mean effective stress as defined by the generalized effective stress approach by Bishop and Blight (1963) in EQ. 3, while further modifications to calculate effective stress may be necessary if utilizing a generalized definition which incorporates air entry suction such as that presented by Khalili and Khabbaz (1998). This increase in mean effective stress could result in additional contraction of the unsaturated soil, similar to a soil specimen subjected to mechanical loading. To evaluate this behavior, the mean effective stress for Tests S-0, US-15, US-20, US-30 and US-40 have been normalized by the initial mean effective stress prior to heating and is shown in Figure 16(b) with temperature. In Figure 16(b), the normalized mean effective stress is observed to remain constant with increasing temperature. This indicates that although decreases in degree of saturation did occur during heating, the change in S was not large enough to cause any significant changes in the mean effective stress. The potential influence of changes in degree of saturation on the normalized mean effective stress was also analyzed for Bourke silt as tested by Uchaipichat and Khalili (2009), and is included in Figure 16(b). Specifically, Uchaipichat and Khalili (2009) reported a shift of the SWRC, as defined by the air entry suction, and its accompanying influence on degree of saturation for compacted Bourke silt at suctions of 0, 100, and 300 kPa for the temperatures of 25, 40, and 60 °C. The data presented by Uchaipichat and Khalili (2009) at a net stress of 200 kPa was reinterpreted in Figure 3(d) to calculate changes in mean effective stress with temperature using the definition of effective stress in EQ. 3. Unlike the results from the Bonny silt tested in this study, the normalized mean effective stress increased with increasing temperature by as much as 8% in the case of the specimen tested at a matric suction of 300 kPa [Figure 16(b)]. Comparison between the normalized mean effective stress results for Bourke silt and Bonny silt suggests soil type may influence the impact of heating on changes in mean effective stress, and potentially the thermal volume change response.

The potential change in mean effective stress due to changes in degree of saturation may also contribute to the overall thermal volume change response of unsaturated silt, in addition to the three mechanisms discussed previously. To examine this hypothesis, the total change in void ratio during heating that is a function of time and temperature, $\Delta e_{total}(t,T)$, was evaluated as a function of the degree of saturation prior to heating for Bonny silt and Bourke silt (Uchaipichat and Khalili 2009) in Figure 17. No apparent trend between these variables is observed. This suggests that the initial degree of saturation may not have a significant effect on the thermal volume change of unsaturated silt when interpreted in terms of mean effective stress. However, it is possible that the degree of saturation may play a more significant role for other soils or compaction conditions where temperature has a greater effect on the SWRC.

Based on the relationships observed between the degree of saturation and thermal contraction during heating, as well as the relative change in mean effective stress in response to decreasing degree of saturation, it can be concluded that another mechanism must be responsible for the thermal volume change of unsaturated soil. The reinterpretation of the results from Towhata et al. (1993) and Burghignoli et al. (2000) in Figure 10 suggests that the thermal volume change response of poorly draining soil is heavily dependent on the recent direction of loading prior to heating. The impact of the previous loading increment on the thermal volume change response of the soil may be related to the secondary compression behavior of the soil immediately following the most recent loading or unloading increment (Burghignoli et al. 2000). In light of these observations, the results from Tests S-0, US-15, US-20, US-30, and US-40 were investigated in reference to the secondary compression index measured prior to heating, $C_{\alpha e}(T_0)$. A schematic showing the definition of the secondary compression index following primary consolidation is shown in Figure 18. The values of the secondary compression index for each test were measured based on the total change in void ratio with time for a duration of 5 hours prior to the start of heating so that a reliable average value could be achieved. Values of $C_{\alpha e}(T_0)$ calculated for each test are shown in Table 4. The total change in void ratio during heating, $\Delta e_{total}(t,T)$, is compared with $C_{\alpha e}(T_0)$ in Figure 19(a). At first glance, a much stronger relationship is observed between $\Delta e_{total}(t,T)$ and $C_{\alpha e}(T_0)$ in Figure 19(a), that between $\Delta e_{total}(t,T)$ and S in Figure 17. Specifically, the total change in void ratio during heating is seen to increase with an increasing secondary compression index measured prior to heating. This suggests the change in void ratio during heating to be influenced by the secondary compression behavior of the soil observed as a response to previous changes in total/effective stress prior to heating. As the Bonny silt specimens were tested in normally consolidated conditions, the thermal volume change tests of

Towhata et al. (1993) have been included for analysis to examine the correlation between secondary compression behavior and thermal volume change for both normally consolidated and heavily overconsolidated soils achieved via loading, unloading, or reloading. The results of this analysis is shown in Figure 19(b). Similar to the results for Bonny silt, an increasing thermal contraction is observed with increasing positive secondary deformations. Furthermore, the thermal deformation for the MC clay appears to follow a similar trend regardless if it is overconsolidated (OC) achieved via unloading or reloading, or normally consolidated (NC). It is proposed the ambient secondary compression behavior prior to heating may serve as a more representative parameter to define the potential thermal volume change response. This is confirmed through the revaluation of the data in Figure 19(b) against overconsolidation ratio as seen in Figure 20 where a much stronger relationship for the total change in void ratio during heating exists with the secondary compression response [Figure 19(b)] than with degree of saturation (Figure 20). Finally, the trend in Figure 19(b) appears to pass near the origin suggesting little to no thermal volume change to occur if the soil is no longer deforming under mechanical secondary compression.

The rate of secondary compression appears to define the potential volume change response of soil during increases in temperature. This may be expected as the transient rate of secondary compression should dominate the measured change in soil volume during heating due to the comparatively low magnitude of thermal expansion of the soil skeleton. Furthermore, when heating at a slow rate, no generation of excess pore water pressure would be expected, reducing the contribution of the primary mechanism of thermal volume change as introduced by Campanella and Mitchell (1968). To further understand the contribution of ambient secondary deformations [e.g., $\Delta e_{\alpha}(t, T_0)$ - A in Figure 18] to the overall change in volume observed during heating [e.g., $\Delta e_{total}(t,T)$ - B in Figure 18], the anticipated change in void ratio due to secondary compression under ambient conditions for Tests S-0, US-15, US-20, US-30, and US-40 was compared with the total change in void ratio measured during heating and is shown in Figure 21(a). As the change in void ratio with time, t, due to secondary compression, $\Delta e_{\alpha}(t,T_0)$, could not be recorded during heating, it can be predicted as follows:

$$\Delta e_{\alpha}(t,T_0) = C_{\alpha e}(T_0) log\left(\frac{t}{t_0}\right) \quad \text{EQ. 8}$$

where t_0 is the initial time of heating, recorded in Table 4. A benefit of this analysis is the ability to reduce the outside influence of time as the duration of heating is expected to impact the total change in volume as a larger increment of time will result in a larger contribution from secondary compression along with any additional deformations induced by heating such as the thermal expansion of the soil constituents (Burghignoli et al. 2000).

A clear linear trend is observed between the total change in void ratio during heating and the anticipated change in void ratio due only to ambient secondary compression shown in Figure 21(a). Specifically, the magnitude of thermal volume change is observed to increase with increasing secondary creep deformation expected for the equivalent time interval. The 1:1 line in Figure 21(a) represents the case where the total change in void ratio during heating is equal to the anticipated change in void ratio due to secondary deformations alone. For data found along the 1:1 line, volume change observed during heating would be solely due to the secondary deformation behavior. In this case, it may be assumed heating leads to no additional change in volume. However, the data in Figure 21(a) falls above the 1:1 line, indicating additional deformations have been induced in the soil during heating. To compare this relationship for several soils, the change in void ratio for Bonny silt from this study, as well as Todi clay from Burghignoli et al. (2000) and MC clay from Towhata et al. (1993) was divided by ΔT and is shown in Figure 21(b) as a function of the values of the secondary compression at room temperature $\Delta e_{\alpha}(t, T_0)$. A consistent trend is observed between the change in void ratio during heating and that expected during secondary deformations for all soil types evaluated. Similar to the results in Figures 19(b) and 21(a), the data is observed to pass through the origin. This observation suggests no significant thermal volume change would be expected for a soil no longer exhibiting mechanical secondary compression and has therefor completed mechanical consolidation in both the primary and secondary stages. In response, it is proposed that the volume change observed during heating is primarily a function of secondary creep in response to mechanical loading and unloading. Further, as the data lays above the 1:1 line [Figure 21(a)], thermal volume change may be observed as an acceleration or increase of the ambient secondary deformation behavior in response to increases in temperature. This observation is confirmed in Figure 22 where the relationship between the total change in void ratio during heating with the anticipated change in void ratio due to secondary compression at ambient temperature is defined, $\Delta e_{total}(t, T)/\Delta e_{\alpha}(t, T_0)$, and compared with temperature. In Figure 22, a value of 1 indicates changes in void ratio during heating to be attributed entirely to secondary compression. For values greater than 1, it may be deduced that heating has contributed an additional change in void ratio along with the expected secondary compression. The ratio $\Delta e_{total}(t, T)/\Delta e_{\alpha}(t, T_0)$ has been evaluated for Tests S-0, US-15, US-20, US-30, and US-40. For comparison, the results of Burghignoli et al. (2000) and Towhata et al. (1993) for Todi and MC clay at various overconsolidation ratios and loading scenarios, respectively, have also been included in Figure 22.

During the initial increase in temperature, an immediate jump in the ratio $\Delta e_{total}(t, T)/\Delta e_{\alpha}(t, T_0)$ is observed. This may be due to the relatively small changes in void ratio measured during initial heating. However, following a change in temperature of approximately 14 °C, the results for all five tests appear to converge to a similar relationship of increasing $\Delta e_{total}(t,T)/\Delta e_{\alpha}(t,T_0)$ with increasing temperature. In addition, the data for Todi and MC clay also appears to follow a similar trend to that found for the Bonny silt. The relationship between $\Delta e_{total}(t,T)/\Delta e_{\alpha}(t,T_0)$ and change in temperature, in Figure 22, suggests the increase in total thermal volume change over that expected via ambient secondary deformations to be controlled by temperature with a larger rate of total volume change occurring at higher temperatures. One potential explanation for the influence of temperature on the rate of secondary compression may involve the impact of temperature on the viscosity of the pore fluid which will be investigated further in the companion paper. Similar to the impact of temperature on the air entry suction, increased temperature will result in a decrease in the viscosity of the pore fluid, resulting in the reduction in interfacial tension between the pore water and soil solids. This reduction in tension may also result in an acceleration of secondary creep due to the reduction as the applied load to the soil transfers to the stronger solid grain to grain contacts.

CONCLUSIONS

This paper presents a critical evaluation of the mechanisms of thermal volume change in saturated and unsaturated soils based on experimental observations from the literature as well as that from an independent experimental investigation performed on Bonny silt. Traditionally, the thermal volume change response of soil has been explained to be a reflection of the initial overconsolidation ratio. However, analysis of the results from the literature suggests thermal volume change to be more dependent on the sign of the most recent change in mean stress prior to heating. Although the conventional mechanisms of thermal consolidation may be useful to explain some experimental observations, a much stronger relationship is observed between the secondary compression behavior and the resulting thermal volume change response for soils with different stress histories. An experimental investigation into the thermal volume change behavior of saturated and unsaturated compacted silt was performed to confirm the influence of secondary compression behavior on thermal volume change. This paper provides an alternate explanation for the role of stress history and the role of loading sequence that may provide more fundamental flexibility in considering thermal volume change than currently adopted by most elasto-plastic models.

ACKNOWLEDGEMENTS

The authors appreciate the support from National Science Foundation grant CMMI-0928159. The views in this paper are those of the authors alone.

REFERENCES

Abuel-Naga, H.M., Bergado, D.T., Bouazza, A. and Ramana, G.V. (2007). "Volume Change Behaviour of Saturated Clays under Drained Heating Conditions: Experimental Results and Constitutive Modeling." *Canadian Geotechnical Journal*. 44: 942-956.

Adam, D. and Markiewicz, R. (2009). "Energy from earth-coupled structures, foundations, tunnels and sewers." *Géotechnique*. 59(3): 229-236.

Alonso, E.E., Gens, A. and Josa, A. (1990). "A Constitutive Model for Partially Saturated Soils." *Géotechnique*. 40(3): 405-430.

Baldi, G., Hueckel, T. and Pellegrini, R. (1988). "Thermal Volume Changes of the Mineral-Water System in Low-Porosity Clay Soils." *Canadian Geotechnical Journal*. 25: 807-825.

Booker, J.R. and Savvidou, C. (1985). "Consolidation around a Point Heat Source." *International Journal for Numerical and Analytical Methods in Geomechanics*. 9:173-184.

Brandl, H. (2006). “Energy Foundations and Other Thermo-Active Ground Structures.” *Géotechnique*. 56(2): 81-122.

Brooks, R.H. and Corey, A.T. (1964). “Hydraulic Properties of Porous Media.” Colorado State University. Hydrology Paper No. 3: 1-27.

Burghignoli, A., Desideri, A. and Miliziano, S. (1995). “Volume Change of Clays Induced by Heating as Observed in Consolidation Tests.” *Soils and Foundations*. 35(3): 122–124.

Burghignoli A., Desideri A. and Miliziano S. (2000). “A Laboratory Study on the Thermomechanical Behaviour of Clayey Soils.” *Canadian Geotechnical Journal*. 37: 764-780.

Campanella, R.G. and Mitchell, J.K. (1968). “Influence of Temperature Variations on Soil Behavior.” *Journal of the Soil Mechanics and Foundation Eng. Division*. 94(SM3): 9-22.

Cekerevac, C. and Laloui, L. (2004). “Experimental Study of Thermal Effects on the Mechanical Behavior of a Clay.” *International Journal for Numerical Analytical Methods Geomechanics*. 28: 209–228.

Coccia, C.J.R. (2015). Mechanisms of Thermal Volume Change in Unsaturated Silt. Ph.D. Thesis. University of Colorado Boulder. Boulder, CO, USA.

Coccia, C.J.R. and McCartney, J.S. (2012). “A Thermo-Hydro-Mechanical True Triaxial Cell for Evaluation of the Impact of Anisotropy on Thermally-Induced Volume Changes in Soils.” *Geotechnical Testing Journal*. 35(2): 227-237.

Coccia, C.J.R. and McCartney, J.S. (2013). “Impact of Heat Exchange on the Thermo-Hydro-Mechanical Response of Reinforced Embankments.” GeoCongress 2013. ASCE. 343-352.

Coccia, C.J.R. and McCartney, J.S. (2016a). “Thermal Volume Change of Poorly Draining Soils II: Model Development and Experimental Validation.” *Computers and Geotechnics*. In Review.

Coccia, C.J.R. and McCartney, J.S. (2016b). “High-Pressure Thermal Isotropic Cell for Evaluation of Thermal Volume Change of Soils.” *Geotechnical Testing Journal*. 39(2): 217-234.

Cui, Y.J., Le, T.T., Tang, A.M., Delage, P. and Li, X.L. (2009). “Investigating the Time-Dependent Behaviour of Boom Clay under Thermomechanical Loading.” *Géotechnique*. 59(4): 319-329.

Cui, Y.J., Sultan, N. and Delage, P. (2000). “A Thermomechanical Model for Clays.” *Canadian Geotechnical Journal*. 37(3): 607–620.

Delage, P., Sultan, N. and Cui, Y.J. (2000). “On the Thermal Consolidation of Boom Clay.” *Canadian Geotechnical Journal*. 37: 343-354.

Demars, K.R. and Charles, R.D. (1982). “Soil Volume Changes Induced by Temperature Cycling.” *Canadian Geotechnical Journal*. 19: 188–194.

François, B. and Laloui, L. (2008). “ACMEG-TS: A Constitutive Model for Unsaturated Soils under Non-Isothermal Conditions.” *International Journal for Numerical and Analytical Methods in Geomechanics*. 32: 1955-1988.

Gens, A. and Olivella, S. (2001). “Clay Barrier in Radioactive Waste Disposal.” *Revue Française de Génie Civil*. 5(6): 845–856.

Ghaaowd, I., Takai, A., Katsumi, T. and McCartney, J.S. (2016). “Pore Water Pressure Prediction for Undrained Heating of Soils.” *Environmental Geotechnics*. 1-9. 10.1680/jenge.15.00041.

Graham, J., Tanaka, N., Crilly, T., and Alfaro, M. (2001). "Modified Cam-Clay Modeling of Temperature Effects in Clays." *Canadian Geotechnical Journal*. 38(3): 608–621.

Houston, S.L., Houston, W.N. and Williams, N.D. (1985). "Thermo-Mechanical Behavior of Seafloor Sediments." *Journal of Geotechnical Engineering*. 111(11): 1249-1263.

Kawai, K., Kato, S. and Karube, D. (2000). "The Model of Water Retention Curve Considering Effects of Void Ratio." *Proceedings of the Asian Conference on Unsaturated Soils*. Singapore. 329-344.

Khalili, N and Khabbaz, M.H. (1998). "A Unique Relationship for χ for the Determination of the Shear Strength of Unsaturated Soils." *Géotechnique*. 48(5): 681-687.

Laloui, L. and Cekerevac, C. (2003). "Thermo-plasticity of Clays: An Isotropic Yield Mechanism." *Computers and Geotechnics*. 30: 649-660.

Laloui, L., Nuth, M. and Vulliet, L. (2006). "Experimental and Numerical Investigations of the Behaviour of a Heat Exchanger Pile." *International Journal for Numerical and Analytical Methods in Geomechanics*. 30: 763-781.

Lee, J. and Znidarčić, D. (2013). "Flow Pump System for Unsaturated Soils: Measurement of Suction Response and the Soil–Water Retention Curve." *Geotechnical Testing Journal*. 36(5): 1-12.

McCartney, J.S., Sánchez, M., and Tomac, I. (2016). "Energy geotechnics: Advances in subsurface energy recovery, storage, and exchange." Computers and Geotechnics. 5(May), 244–256.

McKinstry, H.A. (1965). "Thermal Expansion of Clay Minerals." *The American Mineralogist*. 50: 212–222.

Mitchell, J.K. and Soga, K. (2005). Fundamentals of Soil Behavior. John Wiley & Sons, Inc. Hoboken, NJ.

Mun, W., Coccia, C.J.R. and McCartney, J.S. (2016). “Application of Hysteretic Trends in the Preconsolidation Stress of Unsaturated Soils.” *Journal of Engineering Mechanics.* In Review.

Murphy, K.D. and McCartney, J.S. (2015). “Seasonal Response of Energy Foundations during Building Operation.” *Geotechnical and Geological Engineering.* 32(2): 343–356.

Noorishad, J., Tsang, C.F. and Witherspoon, P.A. (1984). “Coupled Thermal-Hydraulic-Mechanical Phenomena in Saturated Fractured Porous Rocks: Numerical Approach.” *Journal of Geophysical Research*. 89: 365-373.

Paaswell, R.E., 1967, “Temperature Effects on Clay Soil Consolidation,” *Journal of the Soil Mechanics and Foundation Engineering Division*. 93(SM3): 9–22.

Plum, R. L. and Esrig, M. I. (1969). “Some Temperature Effects on Soil Compressibility and Pore Water Pressure.” *Effects of Temperature and Heat on Engineering Behavior of Soils*. Highway Research Board. 103: 231–242.

Romero, E., Gens, A. and Lloret, A. (2003). “Suction Effects on a Compacted Clay Under Non-Isothermal Conditions.” *Géotechnique*. 53(1): 65-81.

Romero, E., Villar, M.V. and Lloret, A. (2005). “Thermo-Hydro-Mechanical Behaviour of Two Heavily Overconsolidated Clays.” *Engineering Geology*. 81: 255-268.

Salager, S., François, B., El Youssoufi, M.S., Laloui, L. and Saix, C. (2008). “Experimental Investigations of Temperature and Suction Effects on Compressibility and Pre-Consolidation Pressure of a Sandy Silt.” *Soils and Foundations*. 48(4): 453-466.

Schiffman, R.L. (1971). “A Thermoelastic Theory of Consolidation.” *In Environmental and Geophysical Heat Transfer*. C.J. Cremers, F. Kreith, J.A. Clark, Eds. ASME. New York. 78-84.

Stewart, M., Coccia, C.J.R. and McCartney, J.S. (2014). “Issues in the Implementation of Sustainable Heat Exchange Technologies in Reinforced Unsaturated Soils.” *ASCE GeoCongress 2014*. Atlanta, USA.

Sultan, N. (1997). *Etude du comportement thermo-mécanique de l'argile de Boom: expériences et modélisation*. Ph.D. Thesis. Ecole Nationale des Ponts et Chaussées. Paris.

Sultan, N., Delage, P. and Cui, Y.J. (2002). “Temperature Effects on the Volume Change Behavior of Boom Clay.” *Engineering Geology*. 64: 135-145.

Tang, A.M., Cui, Y.J. and Barnel, N. (2008). “Thermo-Mechanical Behaviour of a Compacted Swelling Clay.” *Géotechnique*. 58(1): 45-54.

Taylor, D.W. (1942). Research on Consolidation of Clays. Report Serial No. 82. MIT, Cambridge.

Towhata, I., Kuntiwattanakul, P., Seko, I. and Ohishi, K. (1993). “Volume Change of Clays Induced by Heating as Observed in Consolidation Tests.” *Soils and Foundations*. 33(4): 170-183.

Uchaipichat, A. and Khalili, N. (2009). “Experimental Investigation of Thermo-Hydro-Mechanical Behavior of an Unsaturated Silt.” *Géotechnique*. 59(4): 339–353.

LIST OF TABLE CAPTIONS

LIST OF FIGURE CAPTIONS

FIGURE 18: Schematic of primary consolidation and secondary compression due to the change in stress followed by heating (not to scale)

FIGURE 19: Impact of secondary compression index prior to heating on: (a) Total change in void ratio during heating for NC Bonny silt; (b) Total change in void ratio during heating for NC and OC soils – [1] Towhata et al. (1993)

FIGURE 20: Total change in void ratio during heating for NC and OC soils versus overconsolidation ratio – [1] Towhata et al. (1993)

FIGURE 21: Total change in void ratio during heating, $\Delta e_{total}(t,T)$, with the anticipated change in void ratio due to secondary compression, $\Delta e_{\alpha}(t,T_0)$, for: (a) Bonny silt; (b) Bonny silt, Todi clay, and MC clay – [1] Burghignoli et al. (2000); [2] Towhata et al. (1993)

FIGURE 22: $\Delta e_{total}(t,T)/\Delta e_{\alpha}(t,T_0)$ with change in temperature for various soils - [1] Burghignoli et al. (2000); [2] Towhata et al. (1993)

TABLE 1: Summary of geotechnical properties of Bonny silt

Parameter	Value
D_{10}	< 0.0013 mm
D_{30}	0.022 mm
D_{50}	0.039 mm
% Fines smaller than 75 μm	83.9%
% Sand size	16.1%
Liquid Limit, LL	25
Plastic Limit, PL	21
Plasticity Index, PI	4
Activity, A	29
Hydraulic conductivity at saturation, k_s	1.2×10^{-5} m/s

TABLE 2: Summary of soil and testing conditions

Test	**Initial void ratio, e_0**	**Initial dry density, ρ_d**	**Compaction gravimetric water content, w_0**	ψ_{target} **(B)**	p_{target} **(C)**
(-)	(-)	(kg/m^3)	(%)	(kPa)	(kPa)
S-0	0.834	1445	13.9	0	1000
US-15	0.790	1480	13.6	10 and 15	1000
US-20	0.798	1474	14.0	20	1000
US-30	0.810	1464	13.9	30	1000
US-40	0.798	1474	13.9	40	1000

TABLE 3: Saturation results from suction application stage

Test	ψ_{final}	S_{final}
(-)	(kPa)	(-)
S-0	0.00	1.00
US-15	8.9	0.98
US-15	13.9	0.79
US-20	18.6	0.63
US-30	28.6	0.56
US-40	39.4	0.50

TABLE 4: Summary of secondary compression index prior to drained heating

Test Name	$C_{\alpha e}(T_0)$	t_0
(-)	(-)	(hours)
S-0	0.0109	87.8
US-15	0.0183	75.1
US-20	0.0145	76.7
US-30	0.0171	167.0
US-40	0.0091	69.5

Figure 1

Click here to download high resolution image

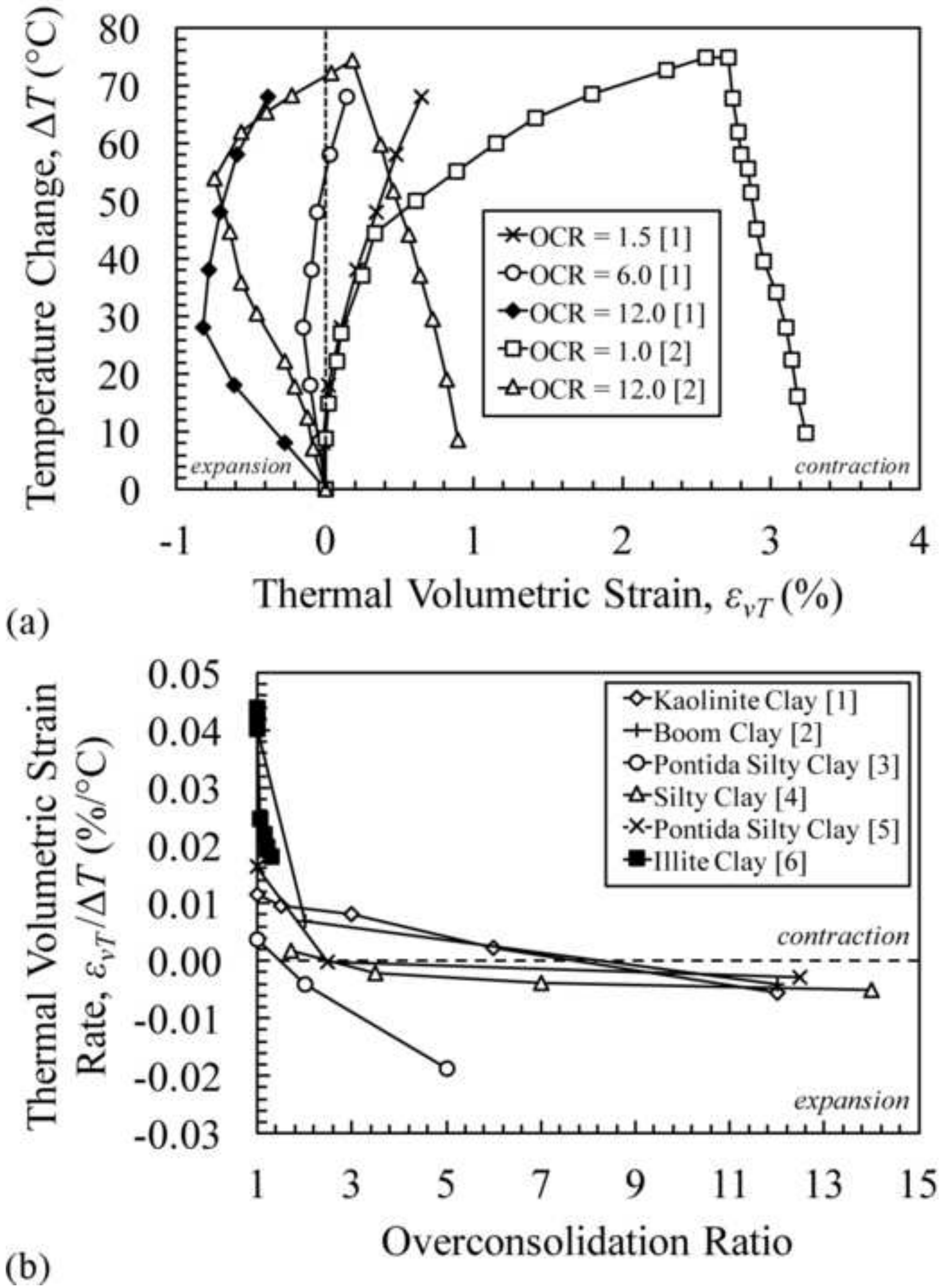

Figure 2
Click here to download high resolution image

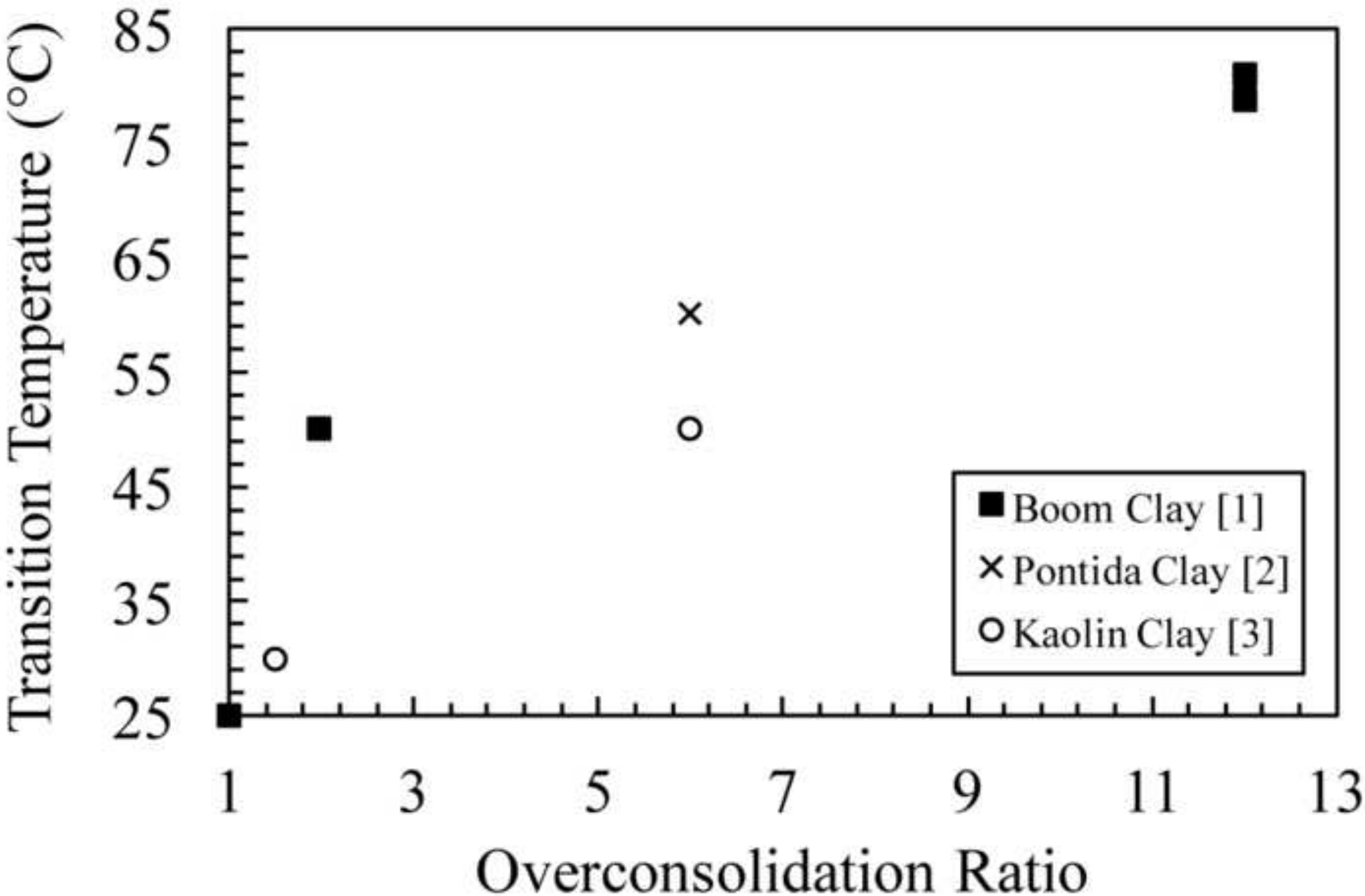

Figure 3
Click here to download high resolution image

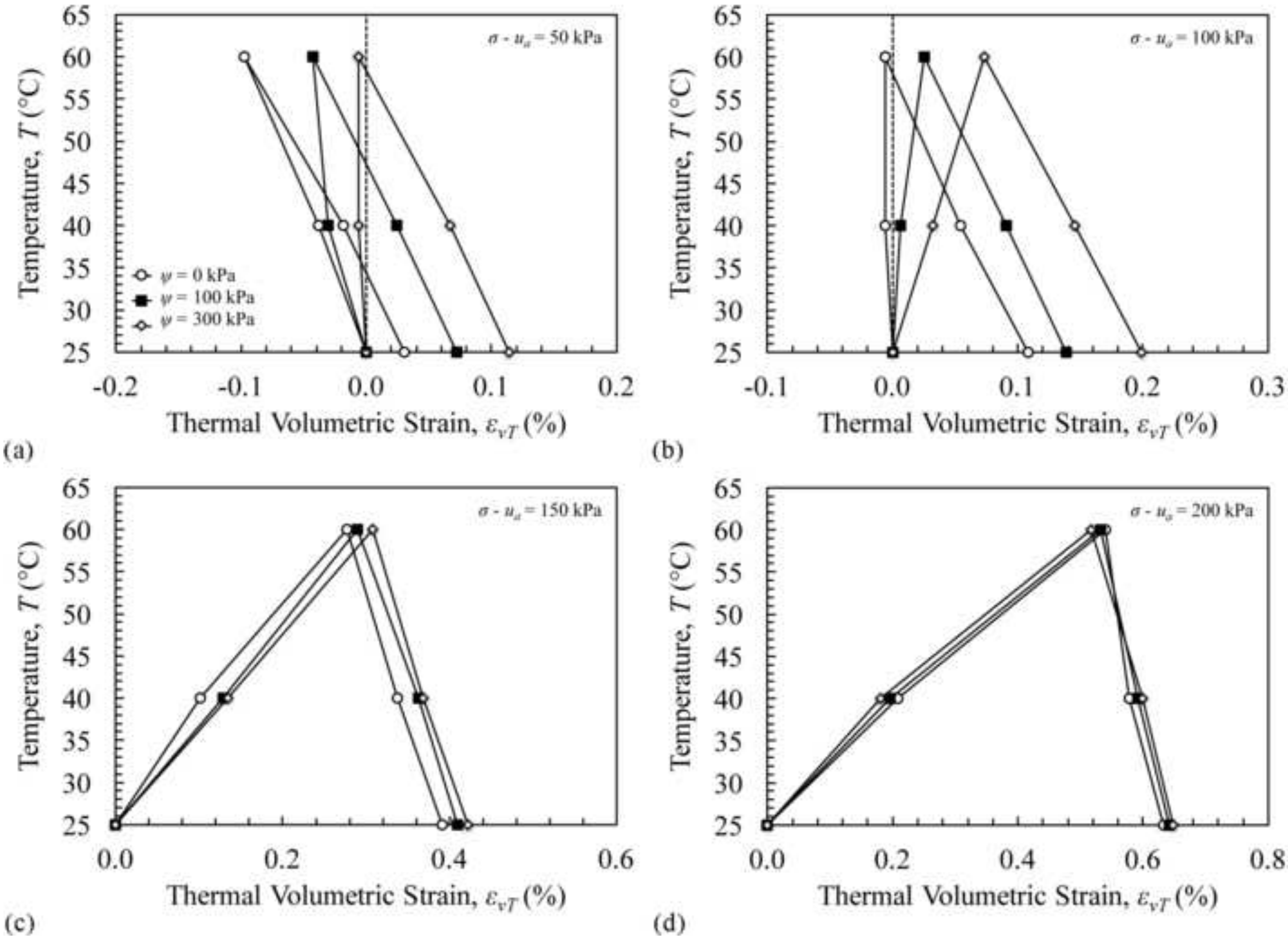

Figure 4
Click here to download high resolution image

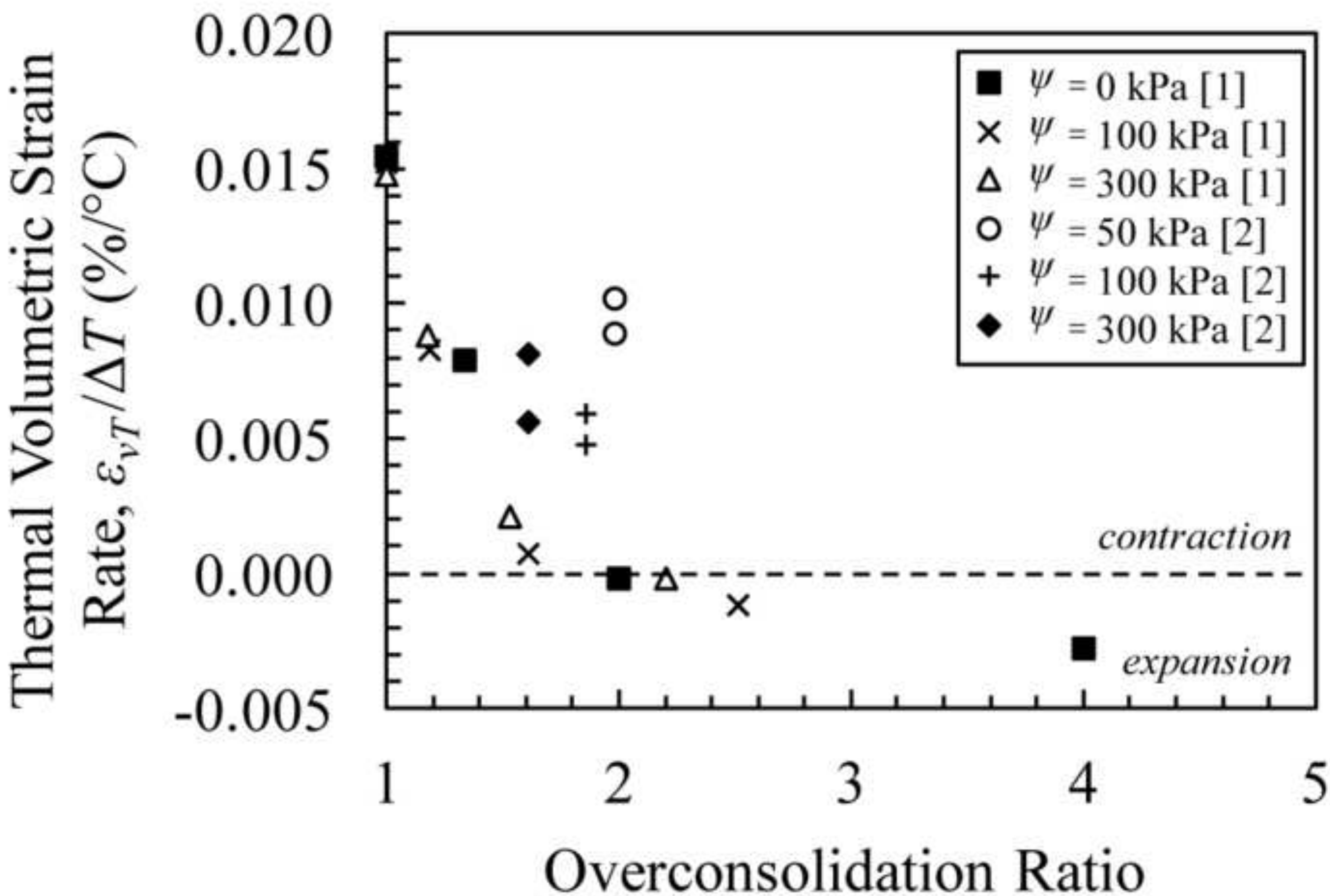

Figure 5
Click here to download high resolution image

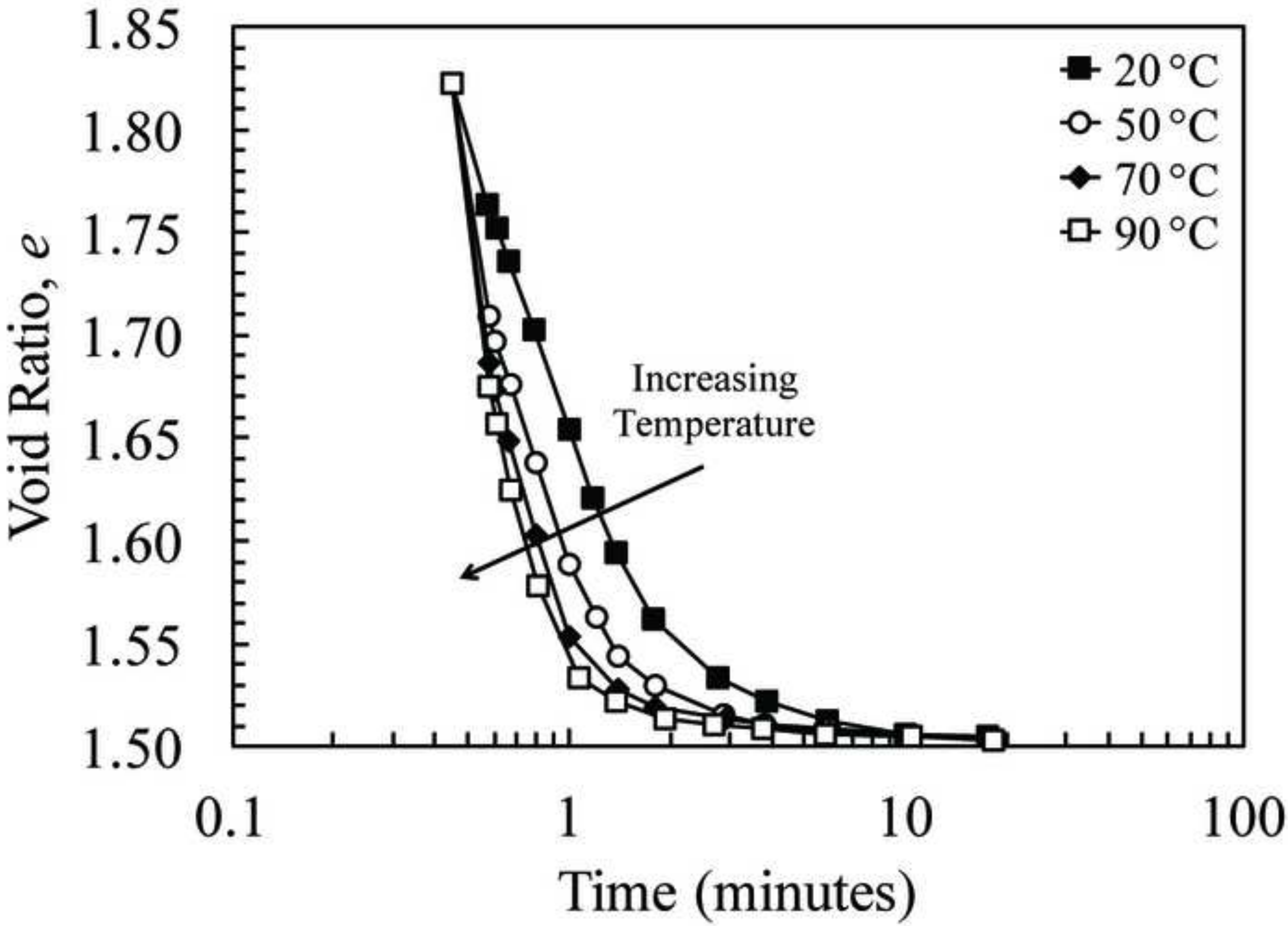

Figure 6
Click here to download high resolution image

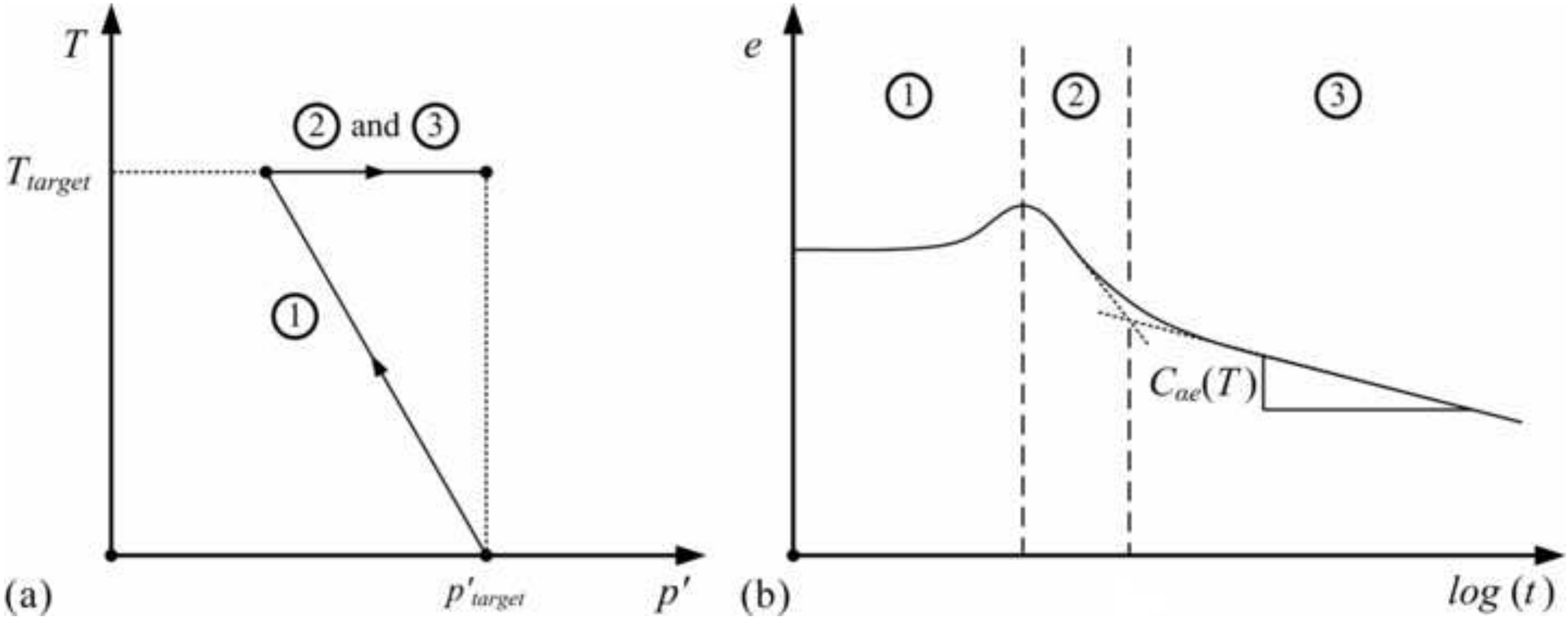

Figure 7
Click here to download high resolution image

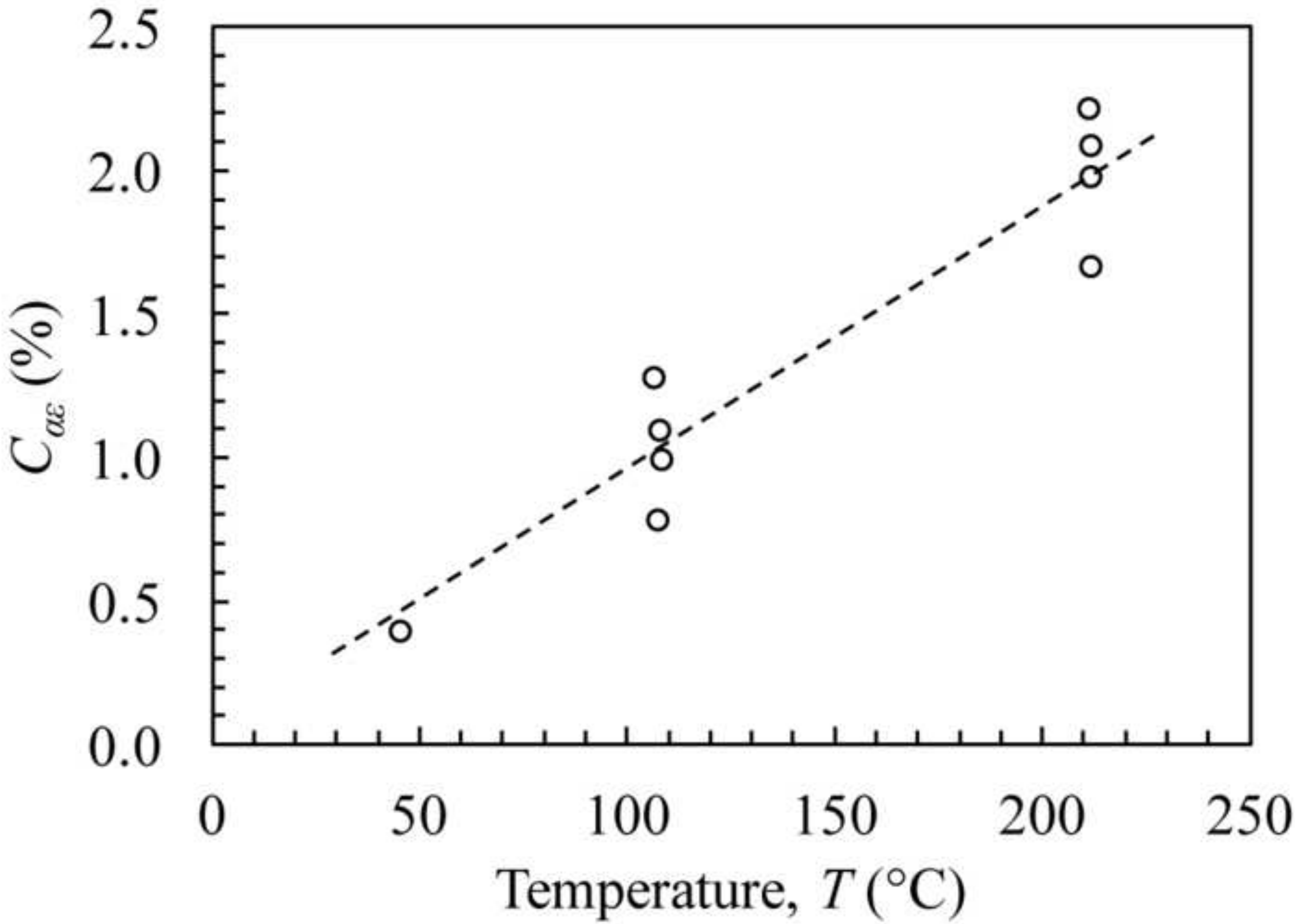

Figure 8
Click here to download high resolution image

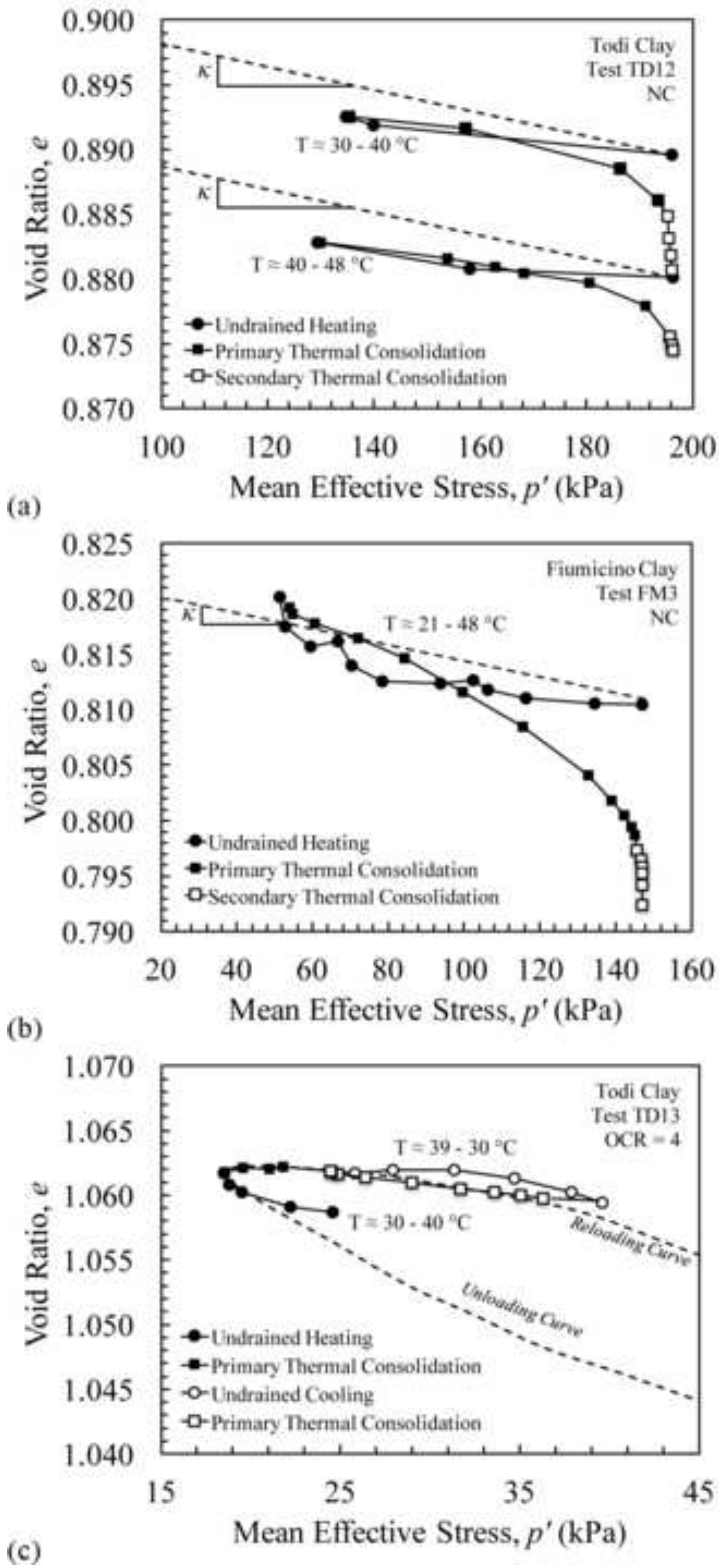

Figure 9

Click here to download high resolution image

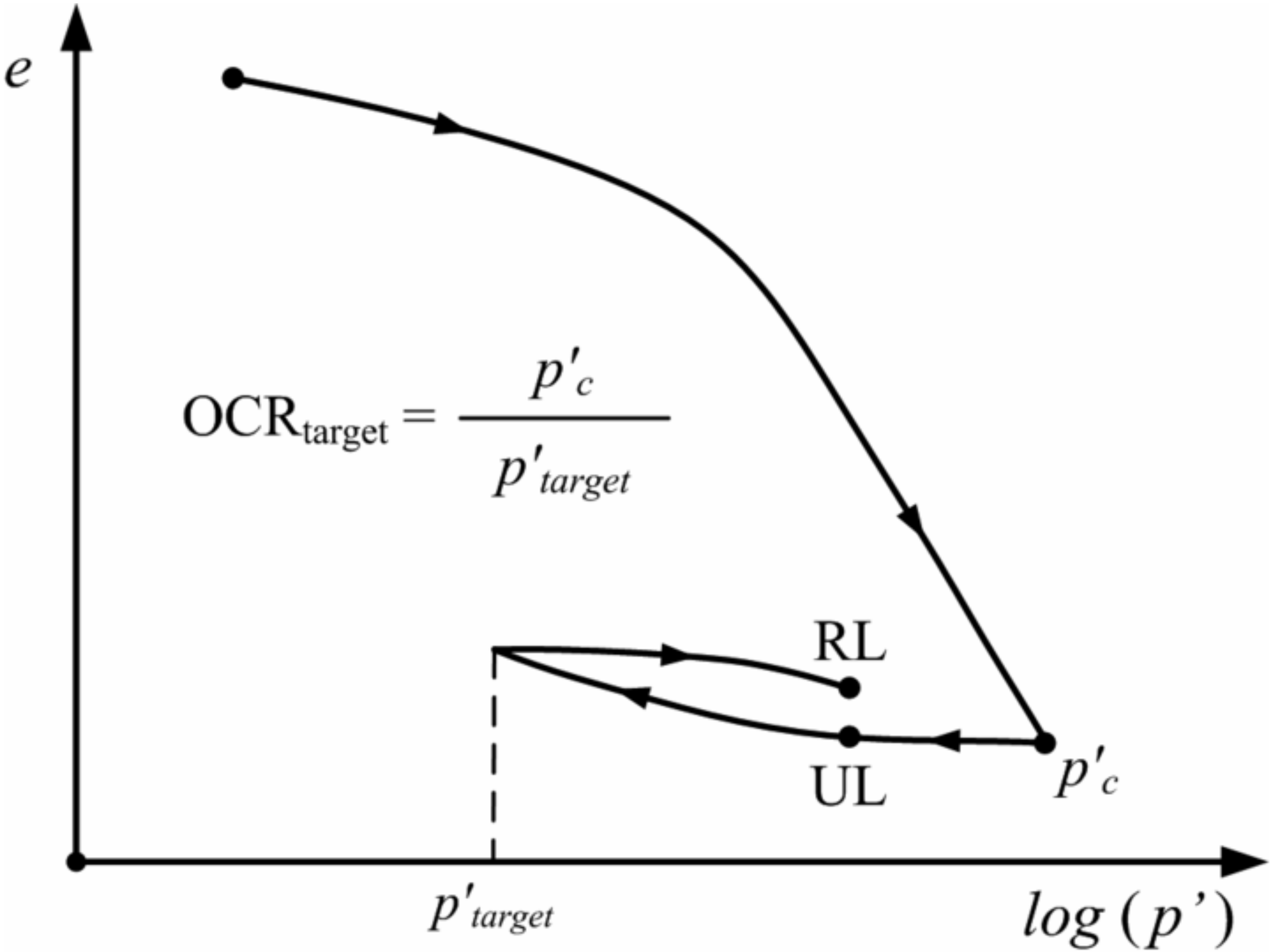

Figure 10
Click here to download high resolution image

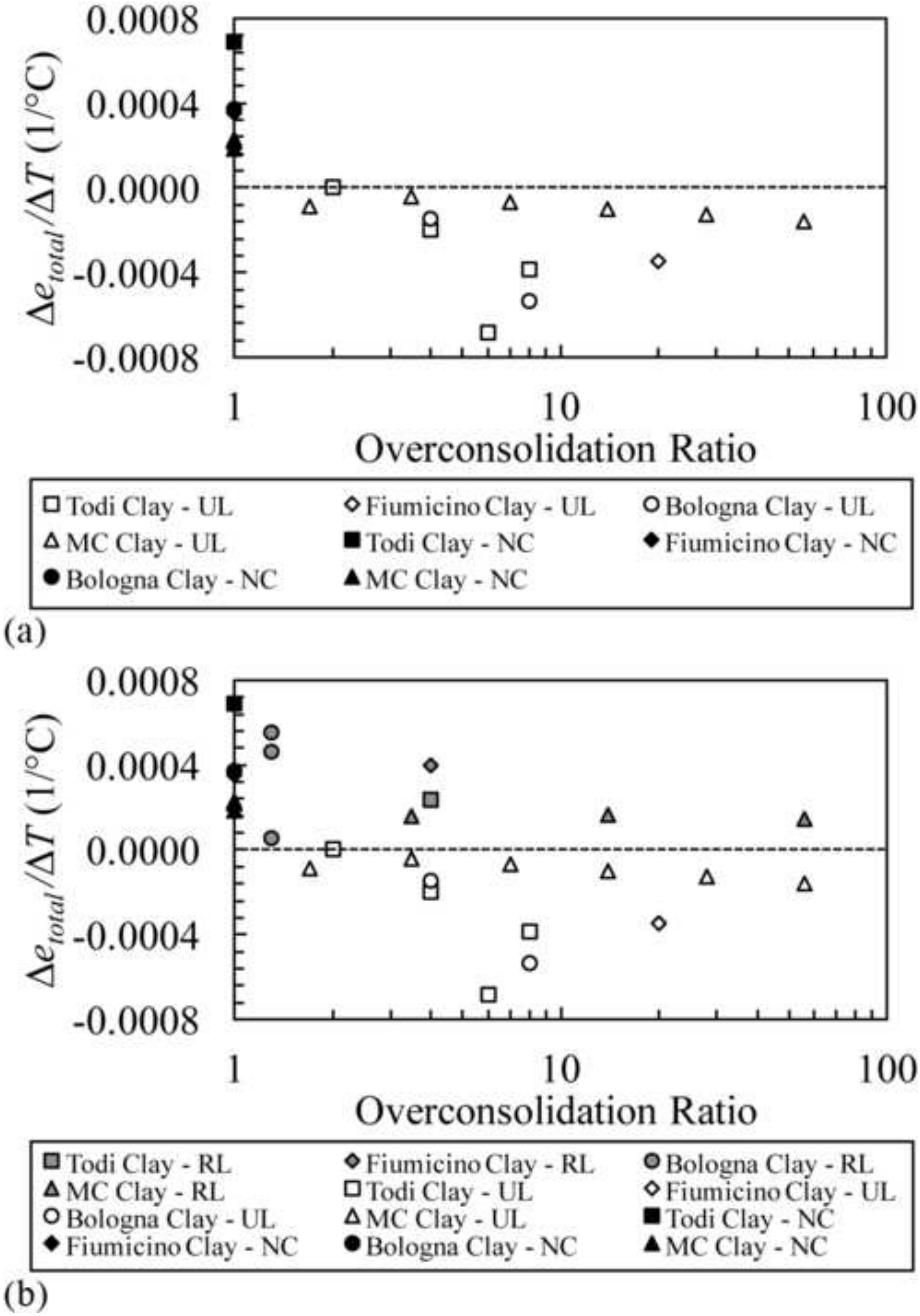

Figure 11

Click here to download high resolution image

A: Soil Specimen; **B:** Top Soil Cap; **C:** Bottom Soil Cap; **D:** Neoprene Membrane; **E:** Coarse Porous Stone; **F:** High Air Entry Value Disk; **G:** DPT (for matric suction); **H:** Thermocouple Probe (bottom); **I:** Thermocouple Probe (top); **J:** Thermal Insulation; **K:** Cell Fluid Bleed Valve; **L:** Circulatory Fan; **M:** Displacement Probes; **N:** Steel Target; **O:** HP Probe Feedthrough; **P:** Cell Pressure Transducer; **Q:** Heating Coil

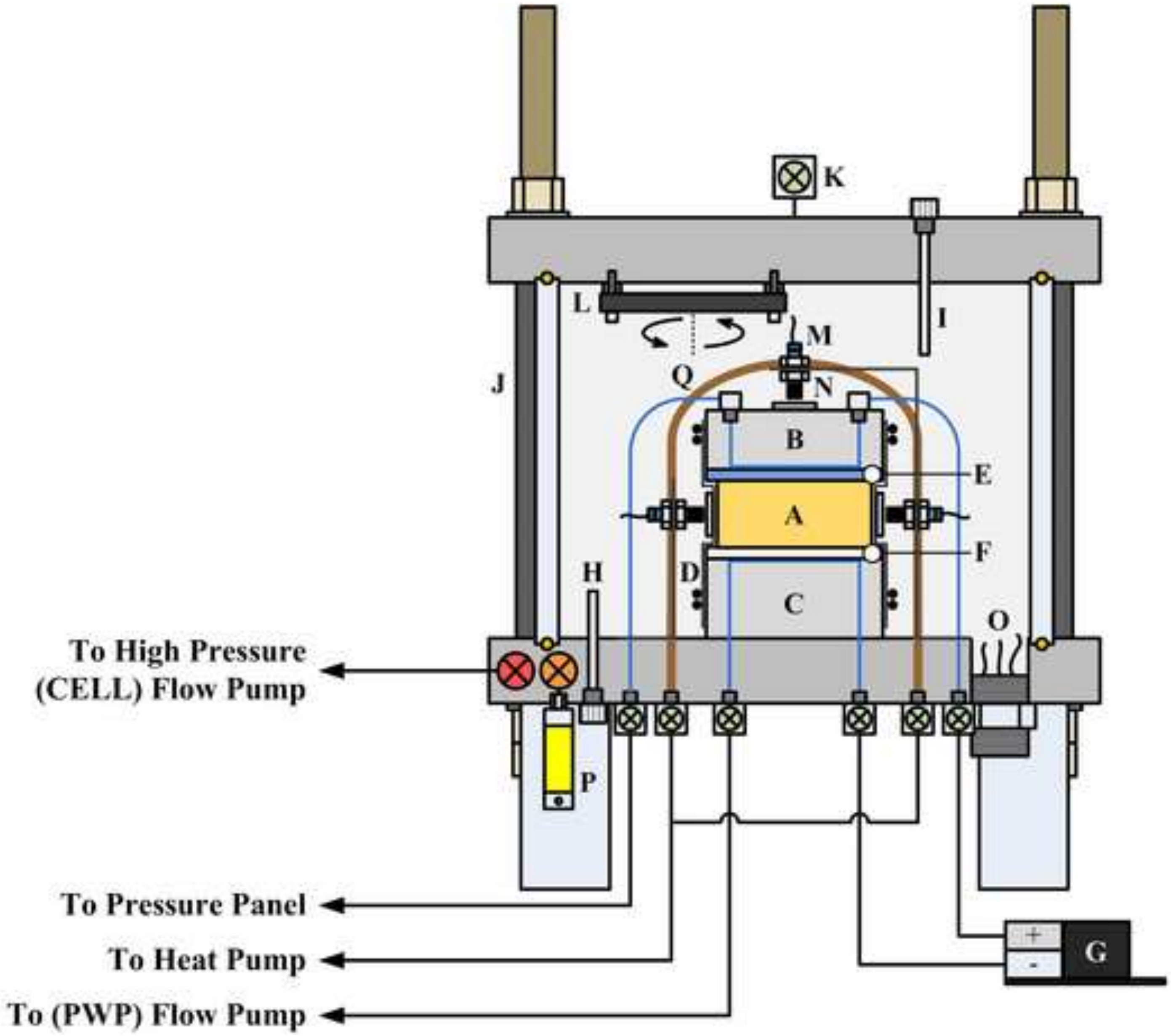

Figure 12
Click here to download high resolution image

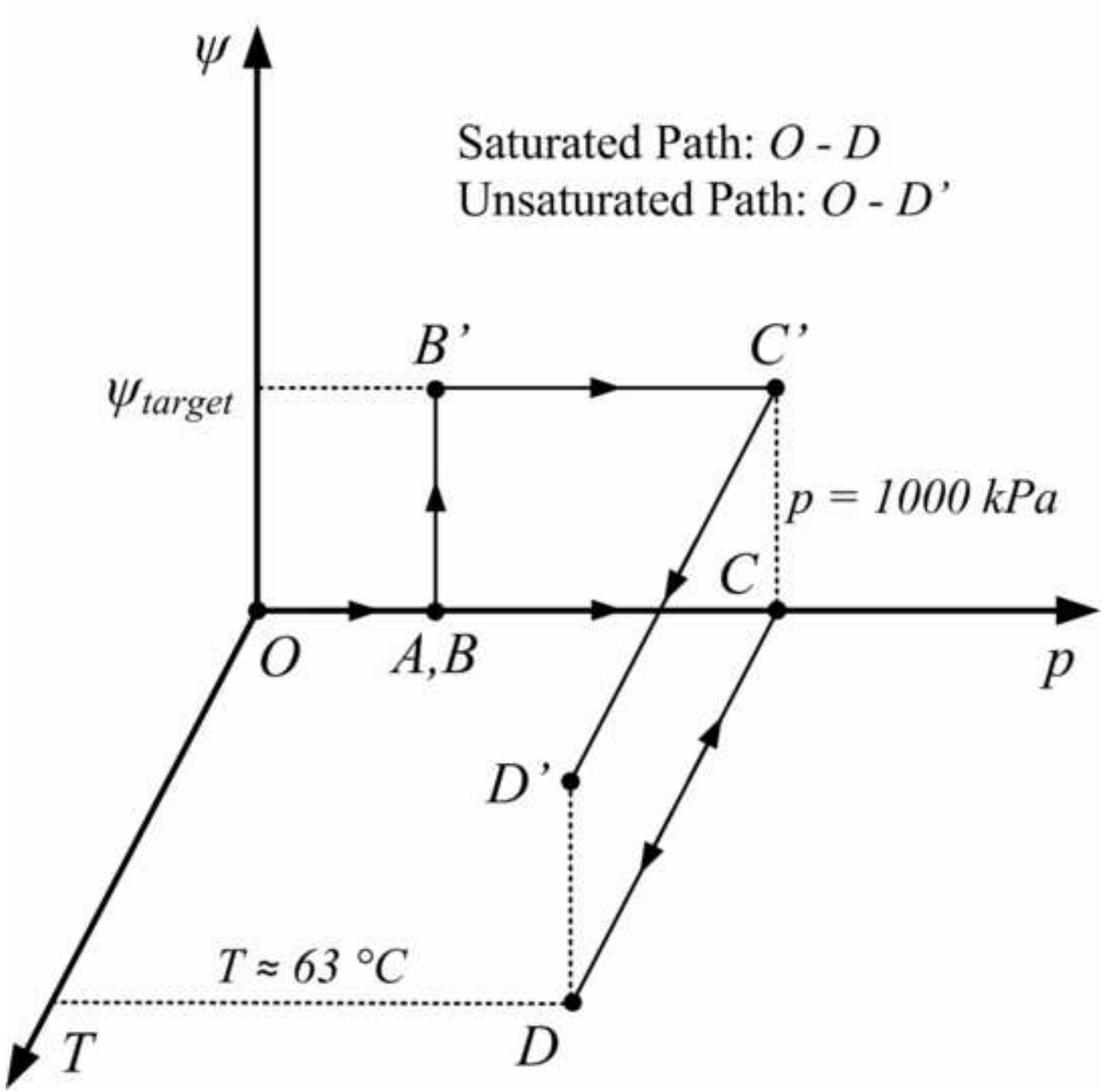

Figure 13
Click here to download high resolution image

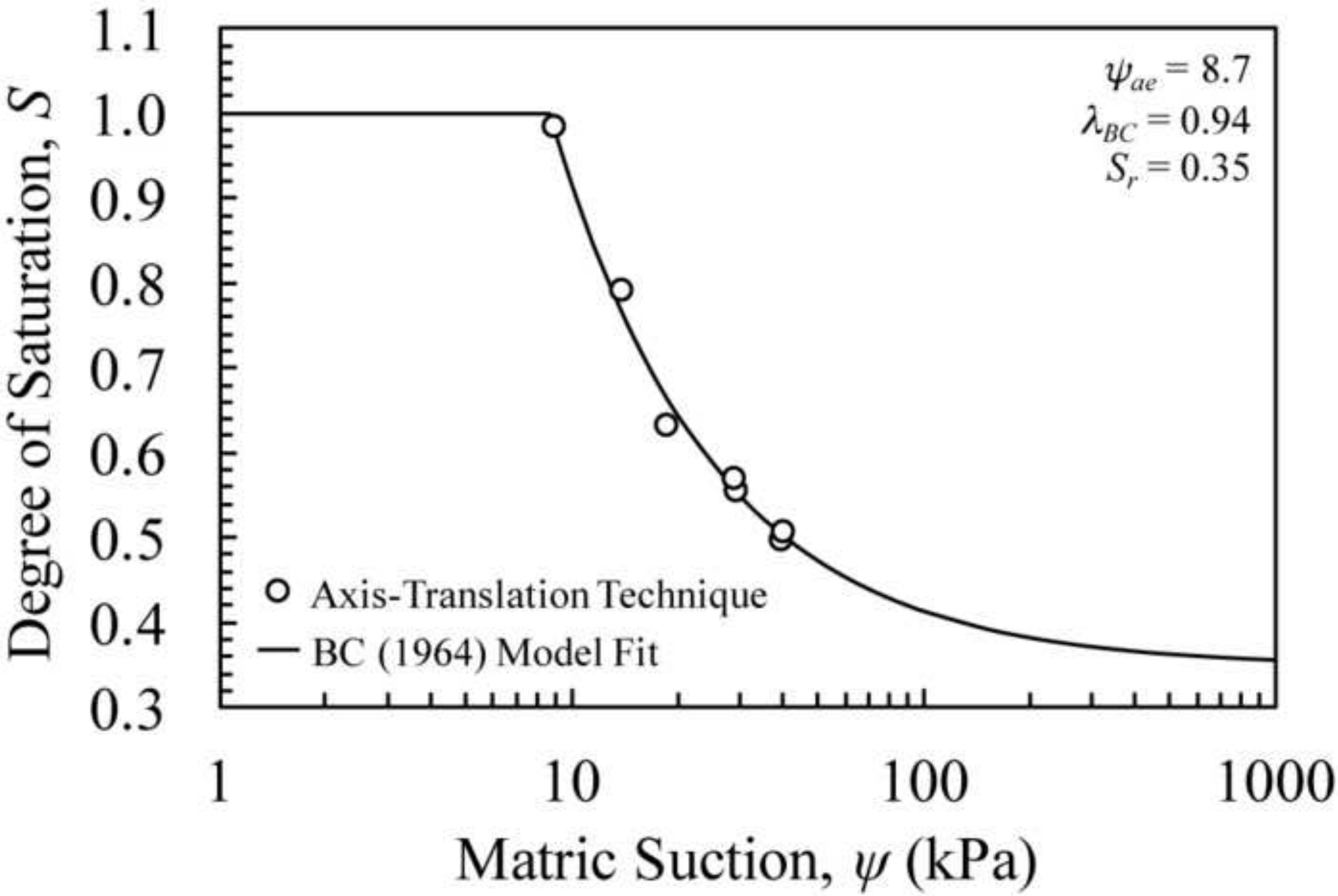

Figure 14
Click here to download high resolution image

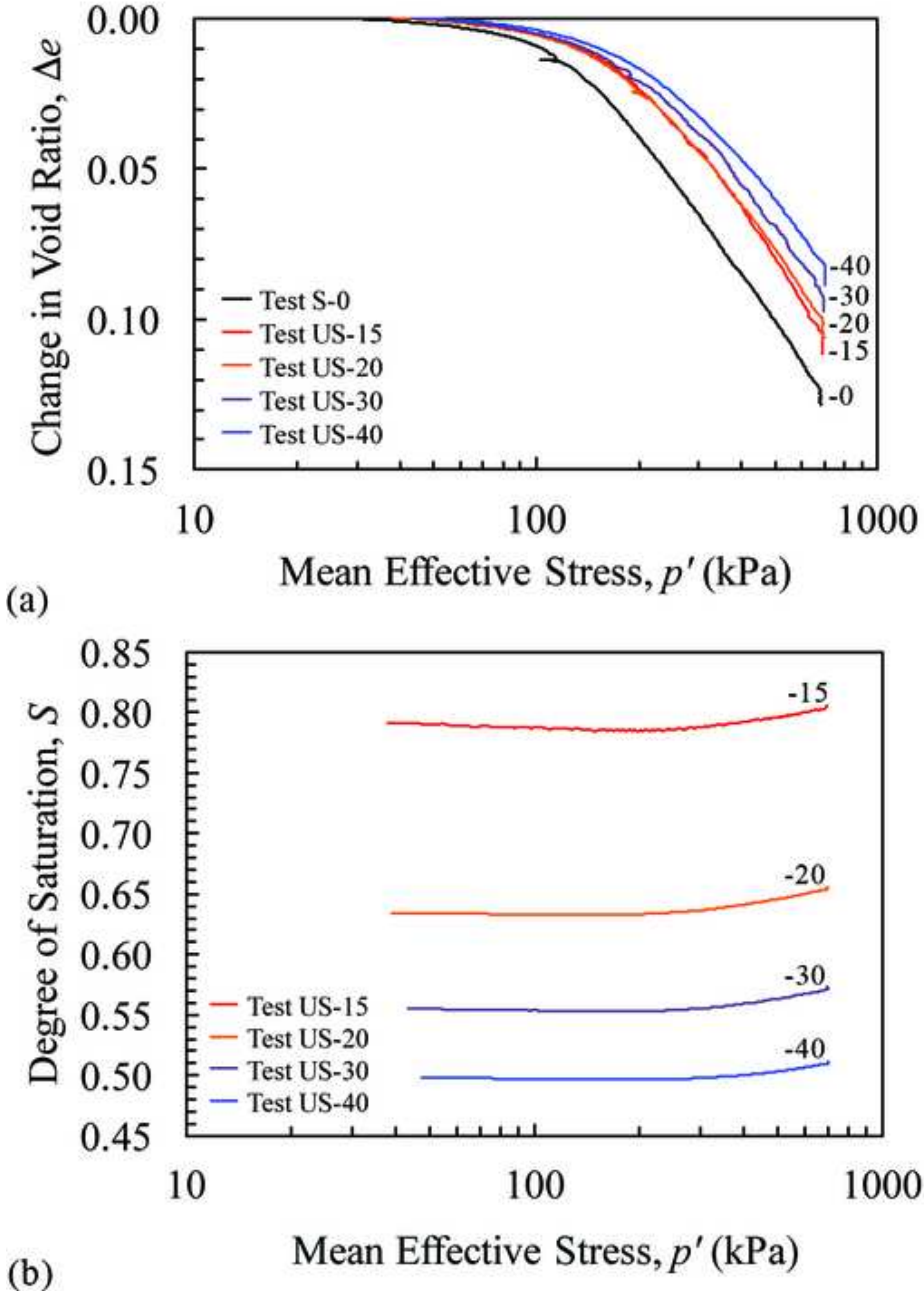

Figure 15
Click here to download high resolution image

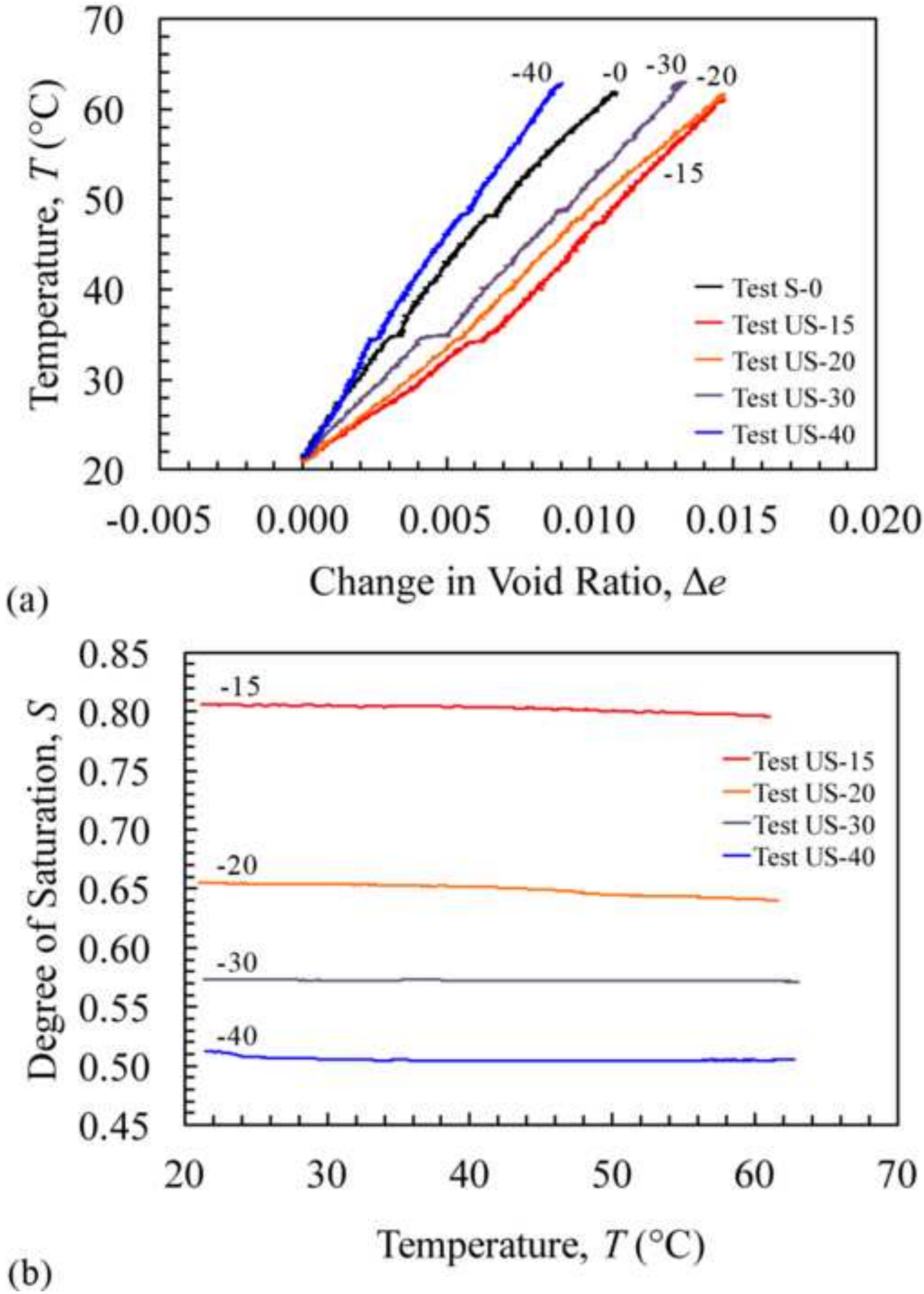

Figure 16
Click here to download high resolution image

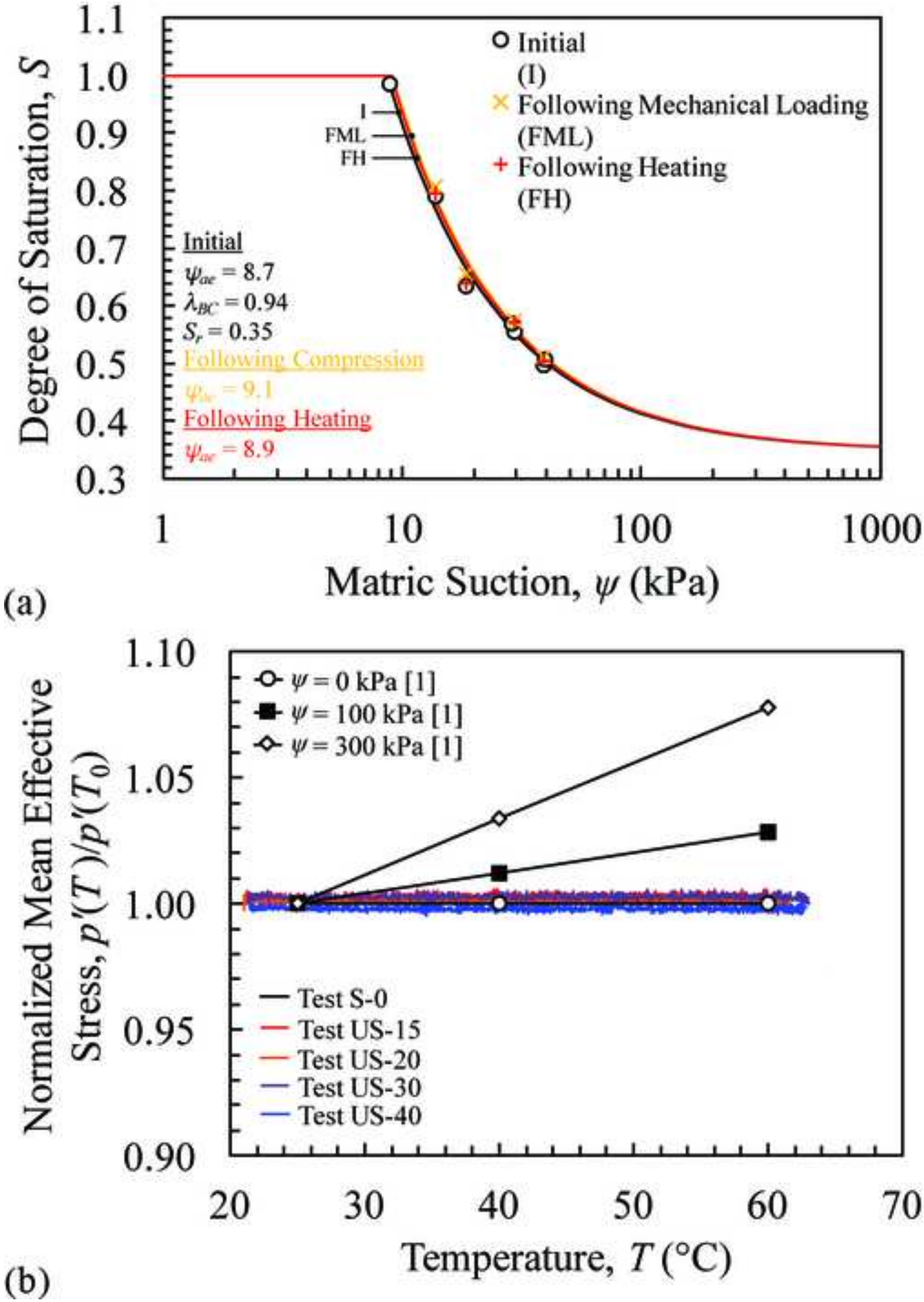

Figure 17
Click here to download high resolution image

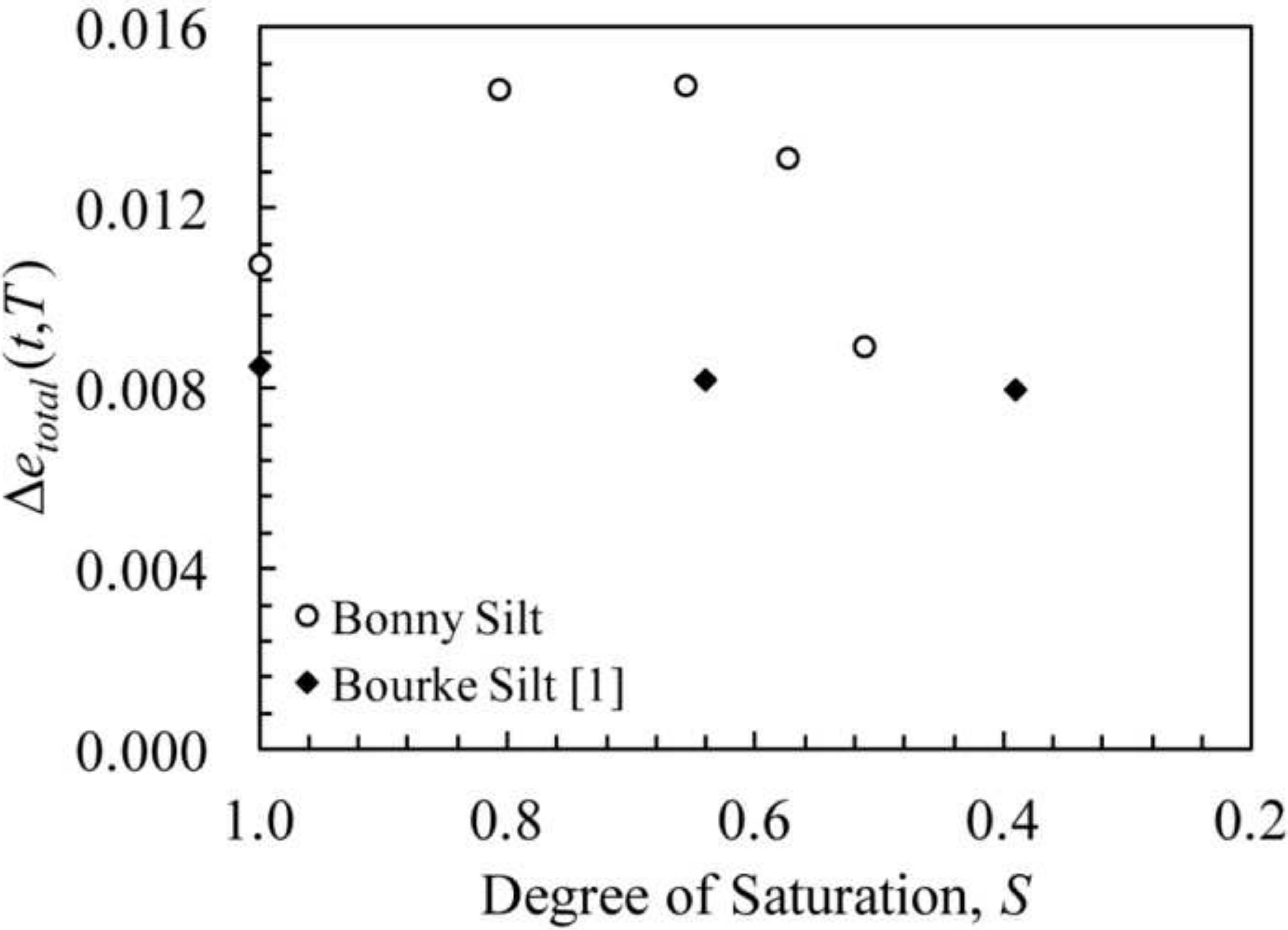

Figure 18
Click here to download high resolution image

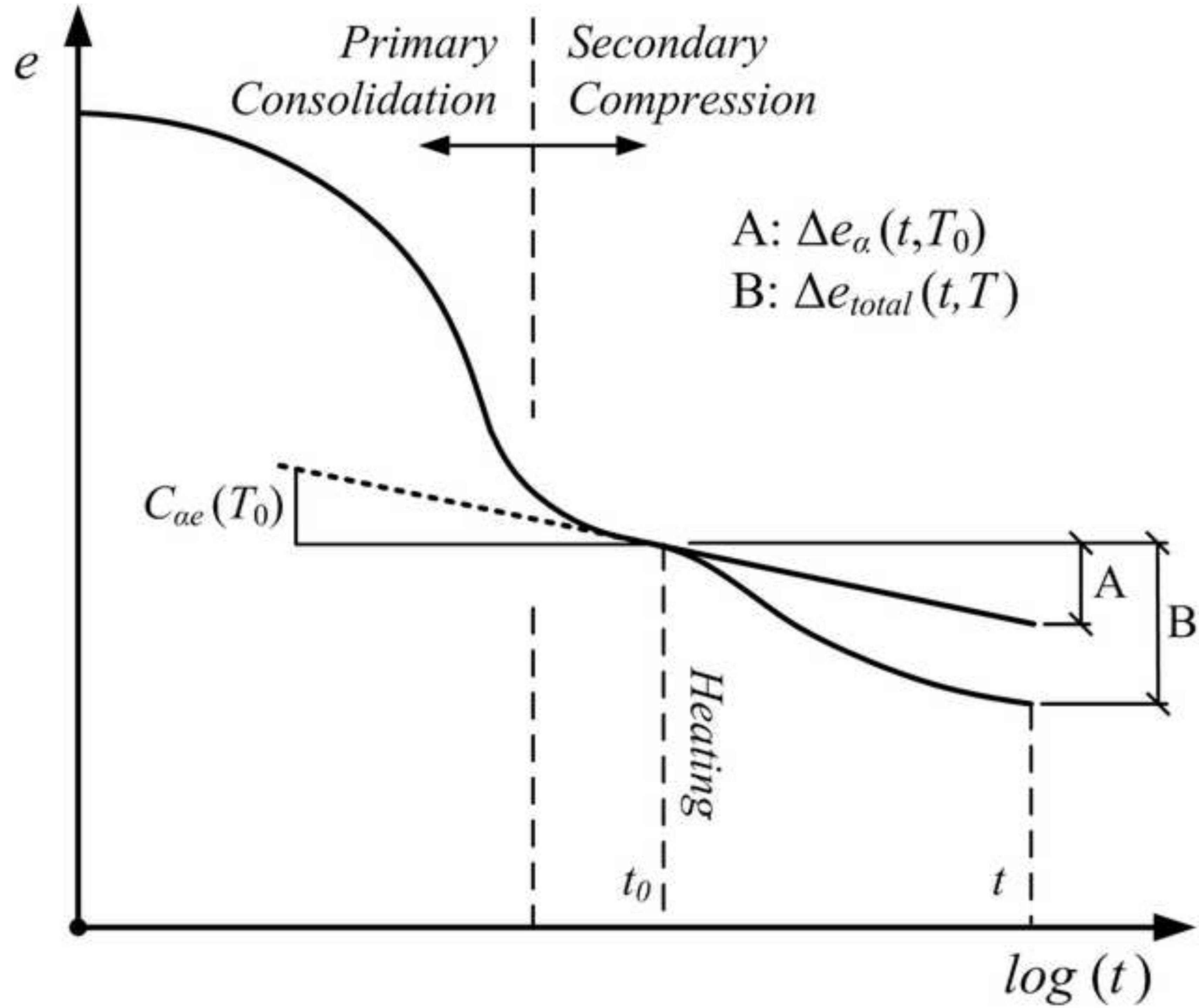

Figure 19

Click here to download high resolution image

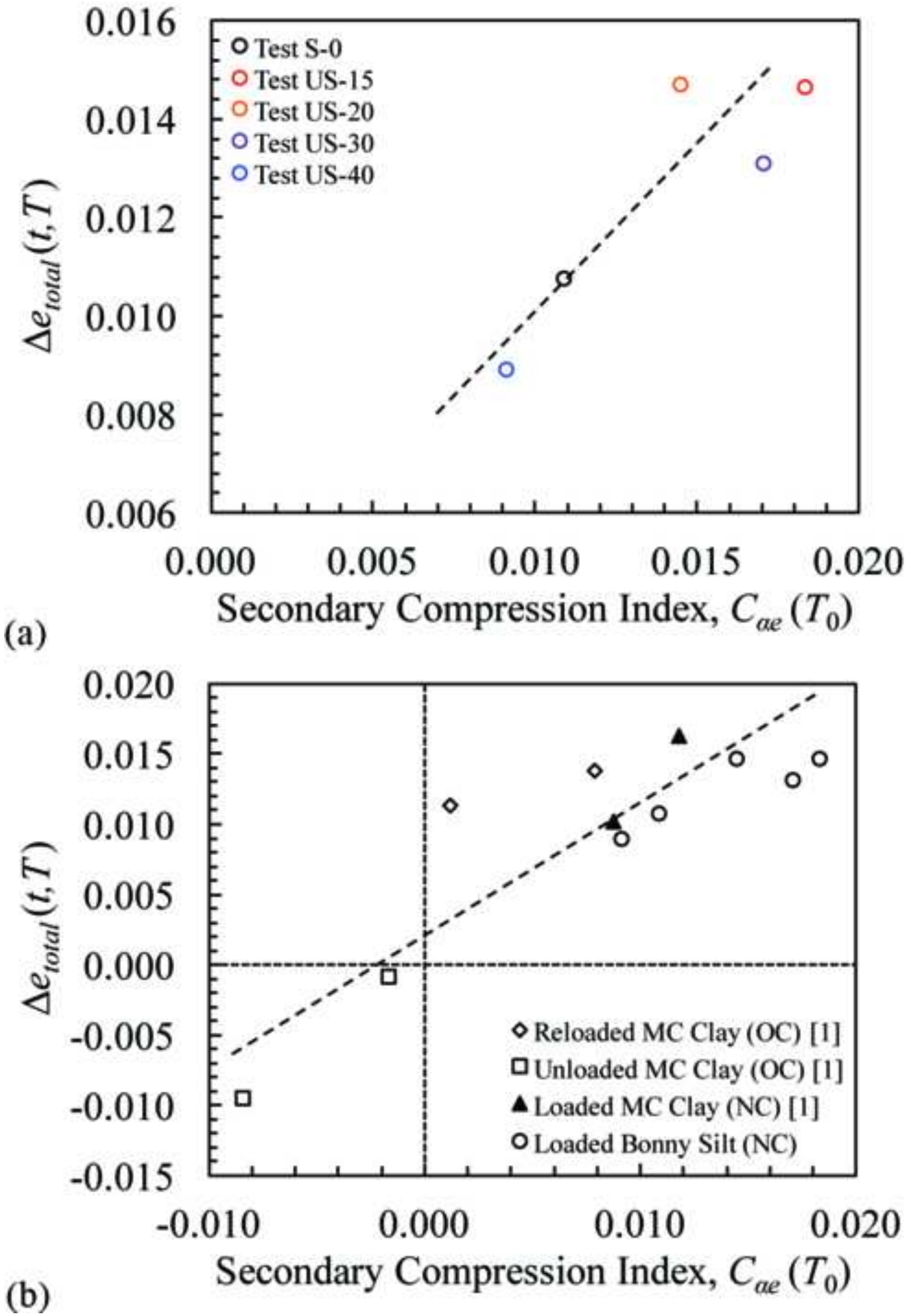

Figure 20
Click here to download high resolution image

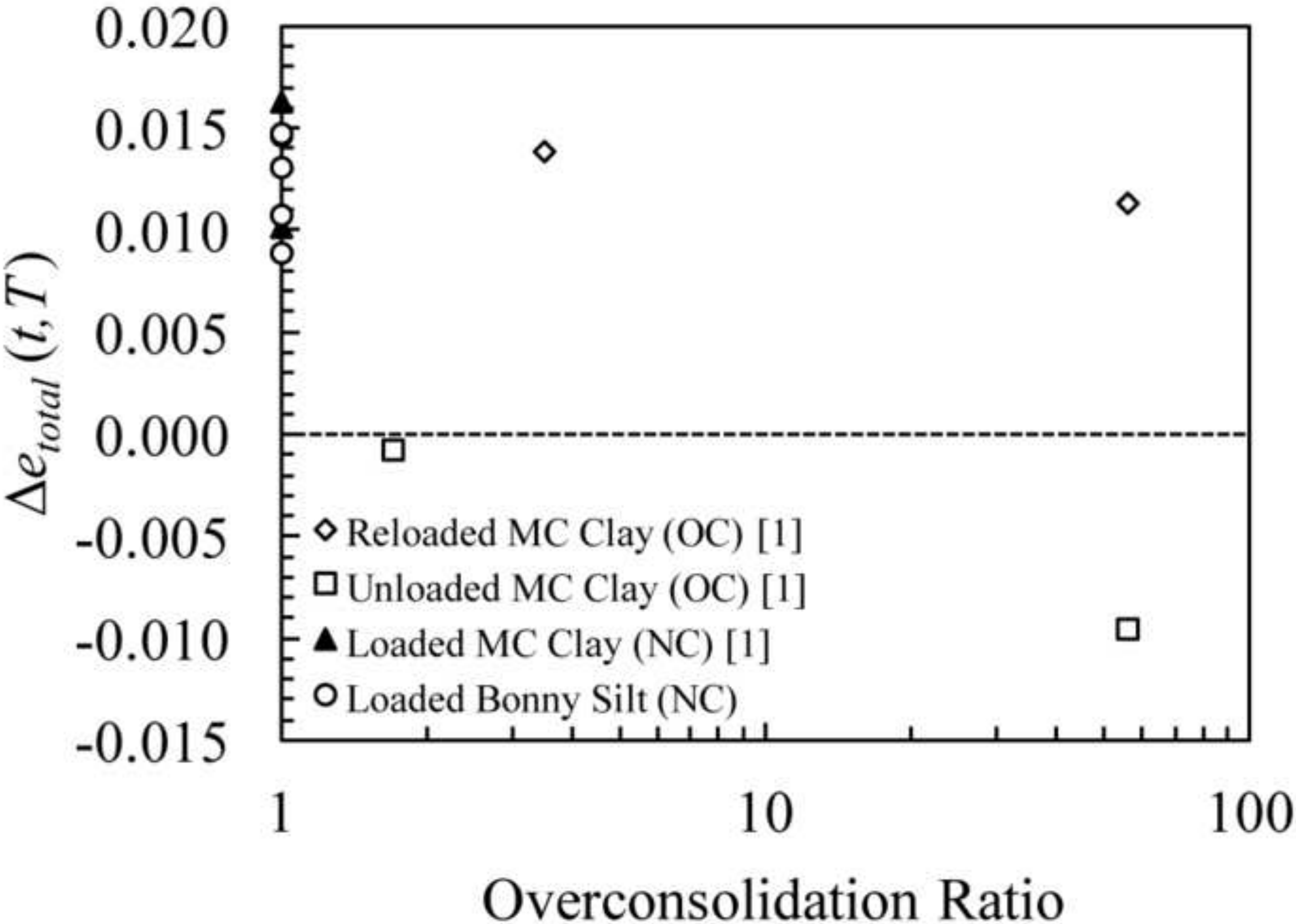

Figure 21
Click here to download high resolution image

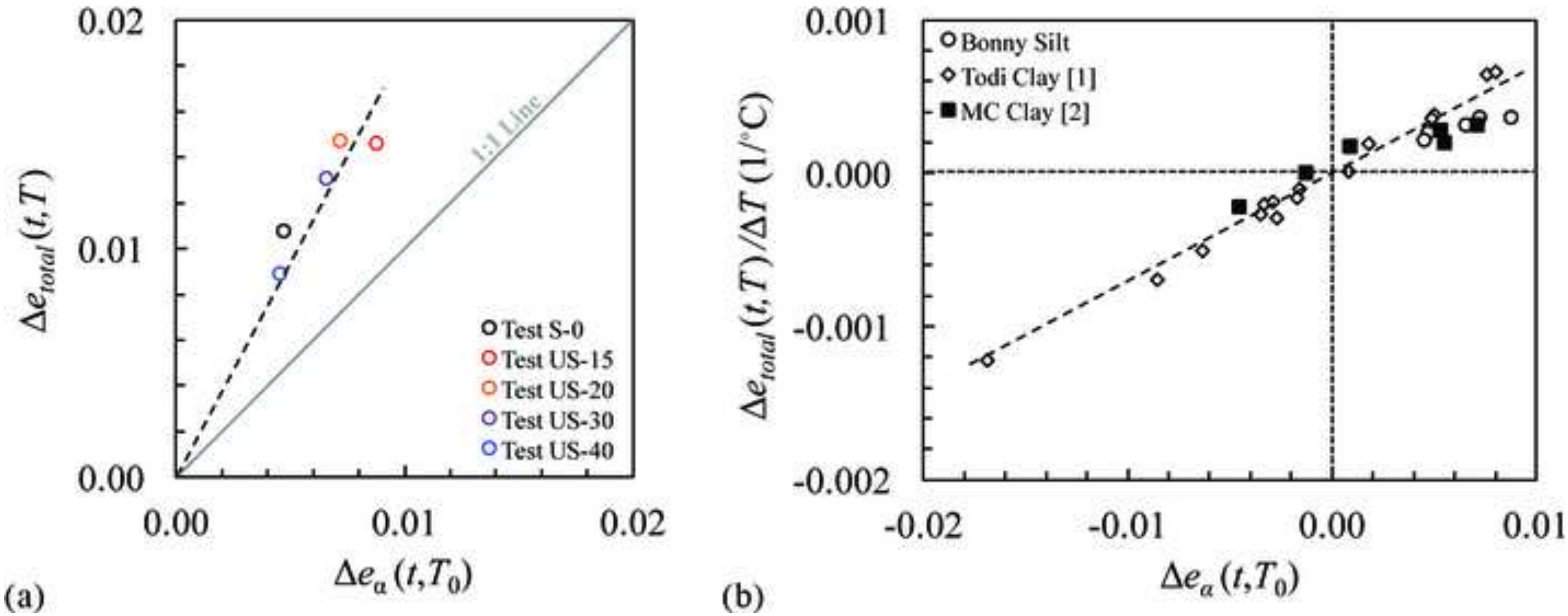

Figure 22
Click here to download high resolution image